In presenting the dissertation as a partial fulfillment of the requirements for an advanced degree from the Georgia Institute of Technology, I agree that the Library of the Institute shall make it available for inspection and circulation in accordance with its regulations governing materials of this type. I agree that permission to copy from, or to publish from, this dissertation may be granted by the professor under whose direction it was written, or, in his absence, by the Dean of the Graduate Division when such copying or publication is solely for scholarly purposes and does not involve potential financial gain. It is understood that any copying from, or publication of, this dissertation which involves potential financial gain will not be allowed without written permission.

7/25/68

A STUDY OF THE DEPENDENCE OF THE ALVEOLAR TO ARTERIAL PRESSURE DIFFERENCE

A THESIS

Presented to

The Faculty of the Division of Graduate

Studies and Research

By

James Arthur Davis

In Partial Fulfillment

of the Requirements for the Degree

Master of Science in Mechanical Engineering

Georgia Institute of Technology

December 1972

A STUDY ON THE DEPENDENCE

OF THE ALVEOLAR TO ARTERIAL PRESSURE DIFFERENCE

Approved:

James M. Bradford Jr., Chairman

Roland H. Ingram Jr.

Walter L. Bloom

William D. McLeod

Date approved by Chairman: 9/14/72

ACKNOWLEDGMENTS

The author wishes to express his appreciation for the helpful advice given by the members of the reading committee: Dr. James M. Bradford, chairman; Roland H. Ingram, MD; Walter L. Bloom, MD; and Dr. William D. McLeod. The author would like to express special appreciation to Drs. Bradford and Ingram for their patience, guidance, and encouragement which made this investigation possible.

He wishes to express his appreciation for the technical assistance received from Miss Lucile Tate and Miss Kathy Moberly, pulmonary technicians at Grady Memorial Hospital. The author would also like to express his gratitude to his wife for her encouragement, patience, and faith, and for the many hours she spent typing the first draft of his thesis.

Finally, the author wishes to thank the Engineering Experiment Station at Georgia Tech, and Dr. Ingram for the support, facilities, and equipment made available for this work.

TABLE OF CONTENTS

TABLE OF CONTENTS (Concluded)

LIST OF TABLES

LIST OF ILLUSTRATIONS

NOMENCLATURE

$AaDO_2$	alveolar to arterial partial pressure of oxygen
FIX	fraction of the gas, X, in the inspired gas mixture (i.e., FIO_2, $FICO_2$)
D	diffusion coefficient
k	a constant in the flow equations, the value of which depends on the units used and desired
k_D	dispersion coefficient
l	variable length
L	fixed length
L_T	transition zone length
M_x	molecular weight of gas x
P	pressure
PaX	Partial pressure of the gas, X in the blood (i.e., PaO_2, $PaCO_2$)
PAX	Partial pressure of the gas, X, in the alveolar (i.e., PAO_2, $PACO_2$)
PIX	Partial pressure of the gas, X, in the inspired gas mixture (i.e., PIO_2, $PICO_2$)
Q	volume flow rate
Q_s	shunt fraction
$\dot{Q}$	perfusion (a flow rate of blood)
r	radial distance
R	radius
R_c	gas constant
t	time

NOMENCLATURE (Concluded)

TL	lag time
TR	rise time
u	velocity
$\bar{u}$	average velocity
u_o	velocity of fluid at the center of the velocity profile
V_x	molecular volume of gas x
$\dot{V}$	ventilation (a volumetric flow rate)
W	mass flow rate
μ	kinematic viscosity
ρ	density

SUMMARY

A study was performed on healthy subjects to investigate the relationship between the alveolar to arterial partial pressure difference of oxygen ($AaDO_2$) and the partial pressure of carbon dioxide in the alveoli ($PACO_2$) and the relationship between the $AaDO_2$ and the partial pressure of oxygen in the alveoli (PAO_2) while breathing a gas mixture with a volume fraction near that of air (20 percent). The $AaDO_2$-$PACO_2$ relationship was studied in two separate procedures. In the first procedure, the $PACO_2$ was varied by changing the breathing rate and tidal volume. In the second procedure, the subject hyperventilated to the lowest $PACO_2$ noted in the first procedure (15 to 20 mmHg) and carbon dioxide was added to the inspired gas mixture until the $PACO_2$ had been varied over the same range as in the previous procedure (approximately 15 to 45 mmHg). During this second procedure, the tidal volume and ventilation rate were maintained at a constant level.

The $PACO_2$ and PAO_2 values were taken from breath by breath analysis of the respired gases performed by a mass spectrometer, assuming the end expired partial pressures of oxygen and carbon dioxide were the PAO_2 and $PACO_2$ values respectively. The blood gas values were measured with an IL313 Blood Gas Analyzer from blood gas samples taken from a radial artery.

Statistical analysis of the data indicated that the $AaDO_2$ correlates better with the PAO_2 than with the $PACO_2$ during the first procedure with varying tidal volume, breathing rate, and PAO_2.

Statistical analysis on the data from the second procedure indicated that the $AaDO_2$ does not correlate with the $PACO_2$ during constant tidal volume, breathing rate, and PAO_2.

A computer program was designed to evaluate the effects of shunting of blood past the lung on the $AaDO_2$ at various levels of PAO_2, and the resulting curve for a 2 percent shunt displayed a good fit to the $AaDO_2$-PAO_2 data found in the first procedure.

CHAPTER I

INTRODUCTION

In a healthy person, there exists a difference between the partial pressure of the oxygen in the alveoli (PAO_2) of the lungs and the partial pressure of the oxygen in the arterialized blood (PaO_2) which has passed by the alveoli. This difference is referred to as the alveolar to arterial pressure difference of oxygen, or $AaDO_2$.

It has been demonstrated that in most patients with pulmonary disorders, the magnitude of the $AaDO_2$ is greater than that found in healthy subjects (1,2). This would indicate that the nature of the pulmonary disorder has in some way affected the efficiency of the lung as a gas exchanging unit.

To understand how the $AaDO_2$ has been affected by a disorder, it is of primary importance to understand what creates the $AaDO_2$, and how it is affected by various physiological factors.

Literature Survey

In an early work, Riley and Cournand (3) discussed an indirect method for determining alveolar partial pressures. The basis for this method is the assumption that the partial pressure of carbon dioxide in the blood ($PaDO_2$) closely approximates the partial pressure of carbon dioxide in the alveoli ($PACO_2$). Once this substitution has been made, the PAO_2 may be calculated by an equation relating PAO_2 to PaO_2, $PaCO_2$, and the venous partial pressures of oxygen and carbon dioxide (3). The

assumption that the $PACO_2$ is equal to the $PaCO_2$ presupposes a uniform distribution of ventilation and perfusion throughout the lung (4).

Later, Riley and Cournand (5) divided the factors contributing to the $AaDO_2$ into four components; air flow to the lung or portions of the lung ($\dot{V}$ - ventilation in liters per minute), blood flow to the lung or portions of the lung ($\dot{Q}$ - perfusion in liters per minute), the amount of ventilation or perfusion which portions of the lung receives (distribution), and limitations to diffusion of oxygen from the alveoli to the blood imposed by the membrane resistance (diffusion limitations). Several more recent investigators have chosen to discuss the effect of three factors in explaining the origin of the $AaDO_2$; uneven distribution of ventilation and perfusion throughout the lung ($\dot{V}/\dot{Q}$ imbalance), shunting of blood past the lung (separated from ventilation and perfusion), and diffusion limitations (6,7).

Figure 1A illustrates the ideal operation of the lung with a two compartment model. With an ideal distribution of ventilation and perfusion to the two compartments, each has the same amount of ventilation and the same amount of blood perfusing the compartment, resulting in the same PAO_2. Moreover, the blood gas partial pressure of the mixed arterial blood is identical to the alveolar partial pressure and the average alveolar partial pressure of oxygen. This model is not, however, consistent with the actual pulmonary system. A more representative model is shown in Figure 1B. Here there is an imbalance in the distribution of ventilation and perfusion (i.e., the $\dot{V}/\dot{Q}$ of the left compartment is less than that of the right), and the alveolar partial pressure of oxygen is neither representative of the average alveolar partial pressure

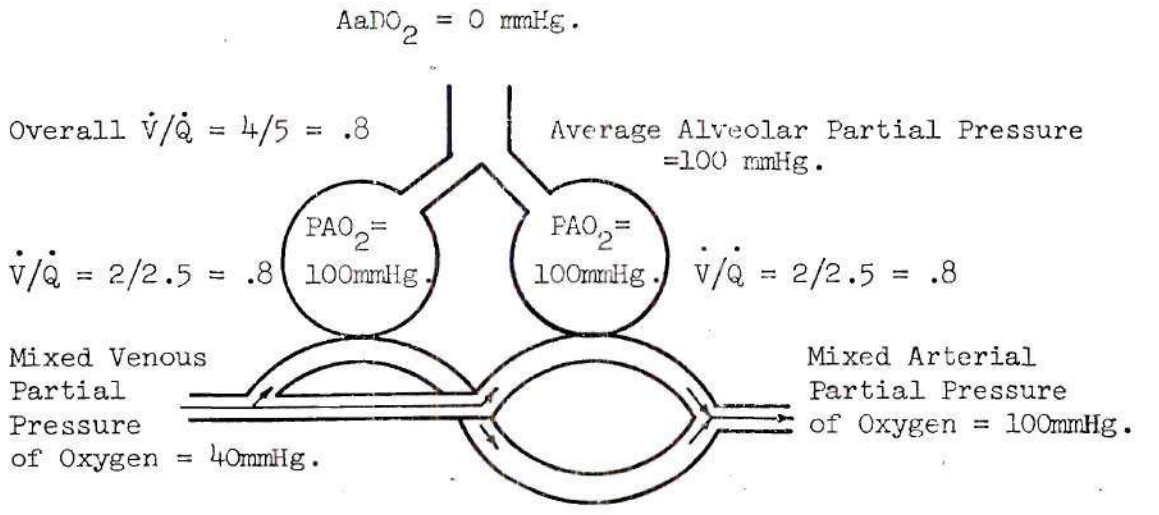

A. Ideal Distribution of Ventilation and Perfusion, (ref. 4).

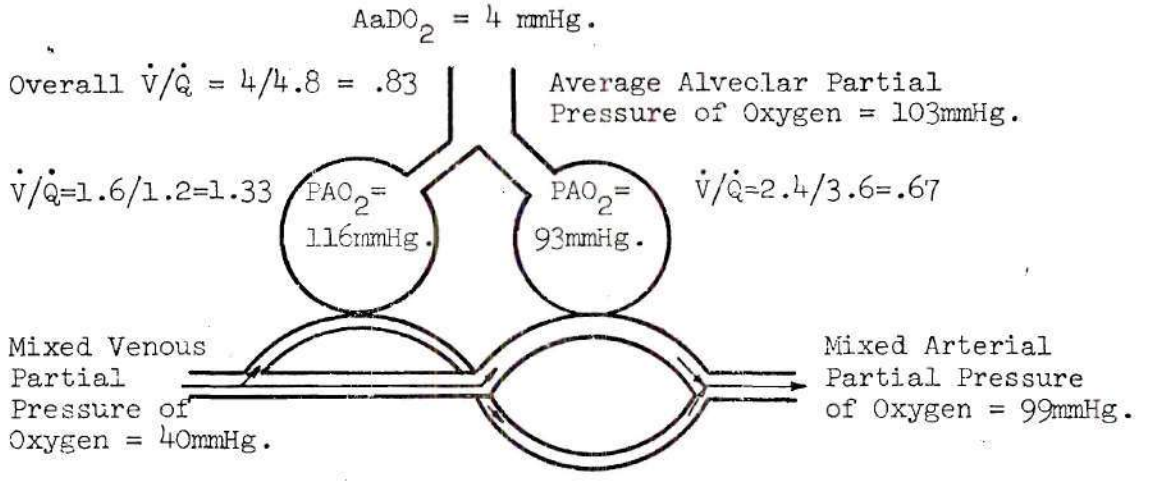

B. Normal Distribution of Ventilation and Perfusion, (ref. 4).

Figure 1. Effect of Uneven Distribution of Ventilation and Perfusion.

or of the mixed arterial partial pressure of oxygen. The average alveolar partial pressure of oxygen represents the combination of the gases in the two compartments in proportion to their respective ventilation. The mixed arterial partial pressure of oxygen represents the PaO_2 characteristic of the oxygen content of the blood passing the two compartments added in proportion to the respective blood flows. Thus, in Figure 1A, the $AaDO_2$ is zero while the $AaDO_2$ in the case of uneven $\dot{V}/\dot{Q}$, illustrated in Figure 1B, is four millimeters of mercury (mmHg). In general, the ventilation to poorly perfused areas of the lung is wasted ventilation and increases the mixed alveolar partial pressure of oxygen where perfusion of poorly ventilated areas of the lung represents wasted blood flow and decreases the mixed arterial blood gas partial pressures of oxygen (4).

Shunting of blood, Figure 2, represents blood which bypasses the lung completely. This venous blood is thus added to the arterial blood, lowering the partial pressure of oxygen in the arterial blood. The contribution of shunting to the total $AaDO_2$ is very difficult to distinguish from the effect of blood flowing through poorly ventilated areas of the lungs while breathing air. However, Riley and Cournand (3) suggested that the effects of shunting and uneven $\dot{V}/\dot{Q}$ can be separated while breathing a gas mixture with a high partial pressure of oxygen (or the fraction of oxygen in the inspired gas, FIO_2, is high). Under this condition the PAO_2 is high, the blood is saturated with oxygen even in the poorly ventilated areas of the lungs, and the effects of the uneven distribution of ventilation and perfusion are negligible (7).

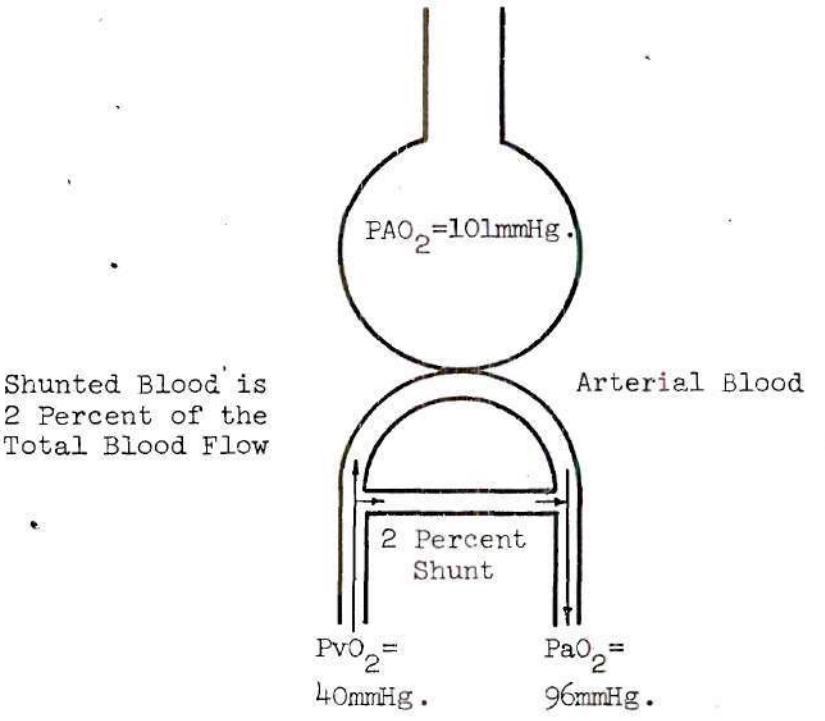

$AaDO_2 = PAO_2 - PaO_2 = 5mmHg.$

Figure 2. Effects of Shunted Blood on $AaDO_2$.

The alveolar membrane presents little resistance to gas exchange between the alveolar gases and the blood gases while breathing air, and contributes little to the $AaDO_2$ (6). Any difference between the PAO_2 and PaO_2 as the result of the membrane resistance is attributed to the diffusion limitation factor.

Much work has been done to isolate and study the effects of these three factors on the alveolar to arterial pressure difference of oxygen (6,7,8,9). Figure 3 shows the theoretical contributions of these three factors to the $AaDO_2$ as discussed by Rahn and Farhi (10,11) assuming a 2 percent shunt, and a log normal distribution of $\dot{V}/\dot{Q}$ around a mean of .85. At low partial pressures of inspired oxygen (PIO_2), the contribution of the diffusion limitation to the $AaDO_2$ becomes of little significance. Breathing pure oxygen, the contribution of true shunting is the primary determinant of the magnitude of the $AaDO_2$, as the contributions of the other factors are insignificant.

From Figure 3, the maximum $AaDO_2$ resulting from the uneven distribution of ventilation and perfusion occurs in a range of PAO_2 in which the $AaDO_2$ due to shunting is increasing and the $AaDO_2$ due to diffusion limitations is decreasing with increasing PAO_2. While breathing air, the $AaDO_2$ is due mainly to the contributions of ventilation-perfusion imbalance and shunting (6).

Recently, Refsum and Kim (2) studied the $AaDO_2$ in patients with various types of pulmonary disease (mainly chronic bronchitis and emphysema) while breathing air. The patients displayed various levels of $PaCO_2$ (determined by blood gas analysis) and PAO_2 (determined by equation in the manner mentioned previously) as a result of the hyper-

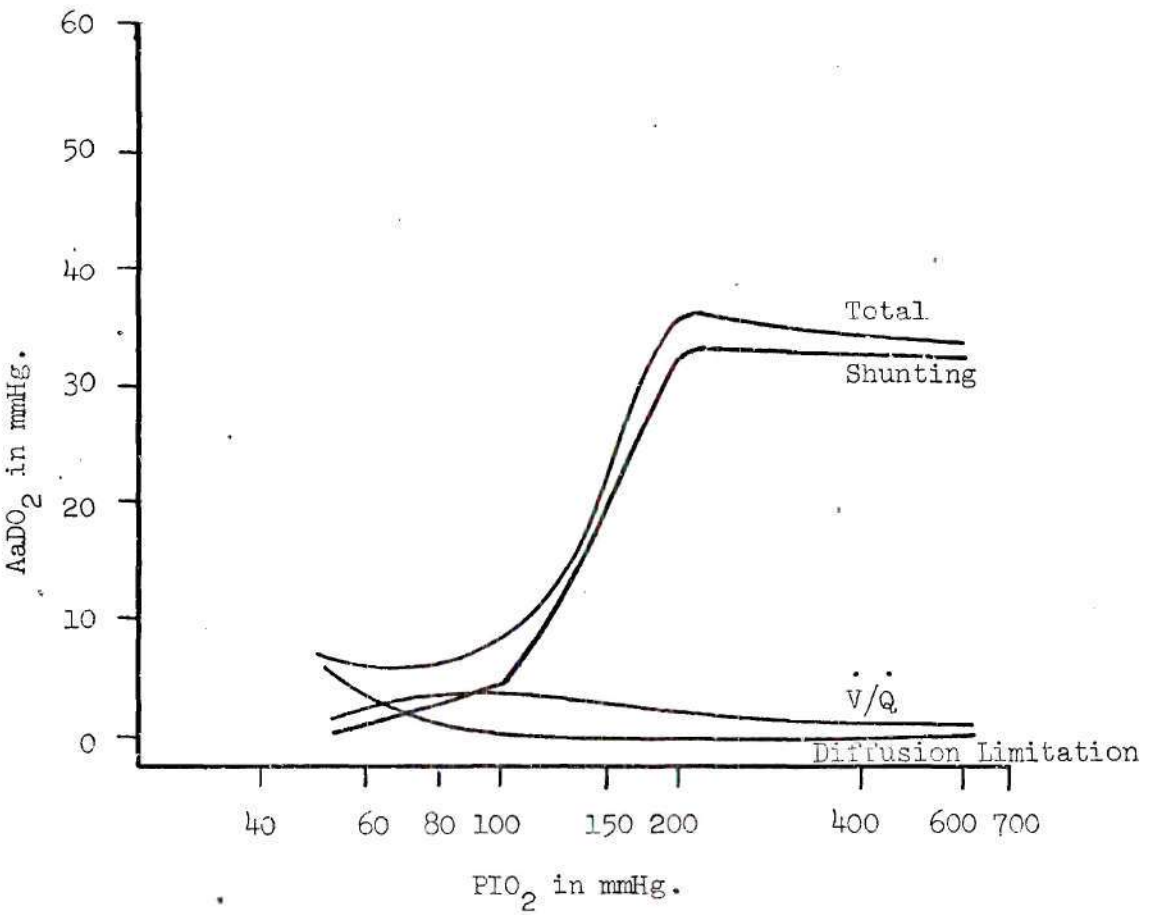

Figure 3. Contribution of Three Factors to the $AaDO_2$, ref. 11.

and hypoventilation attributed to the disorder. The patients were divided into four groups according to the level of $PaCO_2$ displayed during testing, and a trend of decreasing $AaDO_2$ with increasing $PaCO_2$ was noted. They also noted a trend of increasing $AaDO_2$ with increasing PAO_2.

In a later study, Kim and Refsum (12) found the same relationship between the $AaDO_2$ and $PaCO_2$ in nine mechanically ventilated dogs. The increasing trend of the $AaDO_2$ with decreasing $PaCO_2$ (caused by increasing alveolar ventilation) was noted as the tidal volume was increased at a constant breathing rate. The results on the dogs also exhibited the same trend of increasing $AaDO_2$ with increasing PAO_2 as was noted in their previous study (2).

Pichotka, et al. (13) presented the results of a study in which a strong relationship was reported between the $AaDO_2$ and the $PACO_2$, and a weaker relationship between the $AaDO_2$ and the PAO_2. During the study, the arterial blood values were determined by polarographic measurements taken through a hyperamized earlobe. The alveolar partial pressures were determined with the use of a mass spectrometer, assuming that the average alveolar partial pressures were the partial pressures as found in the end expired gases. The variation of the $PACO_2$ and PAO_2 was accomplished by spontaneous hyperventilation. The results exhibited the same trends between the $AaDO_2$ and $PACO_2$ as Kim and Refsum (2,12) noted in their studies between the $AaDO_2$ and the $PaCO_2$.

Equipment Development

Although it was recognized early that the mass spectrometer could be a useful tool in the analysis of respiratory gases, there

was a lack of development in this area (14). Lilly (15), in a 1950 review of methods for continuous gas analysis, pointed out that the sensitivity and accuracy of gas analysis by mass spectrometry could not be matched by any other method of gas analysis. Commercial instruments, however, were expensive and had not been adapted to physiologic studies (15). Siri (16), in 1947, accomplished repetitive scanning and showed that a single mass peak could be recorded with response times in the order of a second. In 1949, Hunter, Stacy, and Hitchcock (17) built a device on the advances made by Nier (18,19). The device could simultaneously monitor oxygen, carbon dioxide, and nitrogen using three collectors spaced in the proper interval. The machine was built to give simultaneous readings on the three gases with a response time in the order of 250 milliseconds. One of the first mass spectrometers used in respiratory research was designed and built by A. O. Nier (20) and used in aid in gas analysis during anesthesia.

Later, K. T. Fowler (21) built a mass spectrometer designed for respiratory research. Fowler combined advances in electronics and mass spectrometry and incorporated the advice of physicians in the design of his device. The result was the first mass produced respiratory mass spectrometer.

In 1971, J. M. Bradford and L. N. Tharp completed construction of the pulmonary Trace Gas Analyzer at the Engineering Experiment Station at the Georgia Institute of Technology. The device used a quadrupole mass spectrometer to analyze the respiratory gases continuously at the lips of the subject. It was this device which was used to monitor the partial pressures of the respiratory gases in this study.

Purpose of the Study

In the studies by Kim and Refsum (2,12), and by Pichotka, et al. (13), the procedures used were such that the $PACO_2$, PAO_2, and the alveolar ventilation were varying simultaneously. From their studies, the authors presented data showing the variation of the $AaDO_2$ with $PACO_2$ and PAO_2.

However, in order to determine the variation of the $AaDO_2$ with $PACO_2$, the PAO_2 and alveolar ventilation must be held constant so that there can be no changes in the $AaDO_2$ caused by changes in PAO_2 and ventilation. The purpose of the present study was to investigate the variation of $AaDO_2$ with $PACO_2$ while holding PAO_2 and ventilation constant. In one series of tests, the $PACO_2$ was varied by changing the degree of hyperventilation as was done in the tests carried out by Pichotka (13). In a second series of tests, the $PACO_2$ was varied over the same range as in the first series by adding carbon dioxide to the inspired gas mixture while holding the PAO_2 and ventilation rate constant.

CHAPTER II

EQUIPMENT

The Pulmonary Trace Gas Analyzer

In the short history of the respiratory mass spectrometer, the basic scheme has not been altered greatly. The basic idea, shown in Figure 4, is to withdraw a continuous sample of respiratory gases at the lips of the subject into a mass spectrometer for analysis. The variations in the design of the respiratory mass spectrometer have dealt mostly with the mass spectrometer itself. As mentioned previously, the early devices used such methods as rapid scanning and fixed multiple collectors in magnetic sector type mass spectrometers to achieve a continuous reading on the respiratory gases of interest. More recent devices have used various types of mass spectrometers using methods such as independently moveable, multiple collectors (22), and electronic advances to give continuous, multiple gas readings.

The Pulmonary Trace Gas Analyzer is of the same basic design as previous respiratory mass spectrometers. The vacuum system draws the sample through the sampling system to the inlet of a quadrupole mass spectrometer. The quadrupole analyzes the gas for the component of interest and the signal is relayed to the recorder. Under normal operation, the quadrupole continuously scans any set mass range at high speeds. It also has the ability to be programmed for monitoring continuously any single mass. Using four separate programming channels,

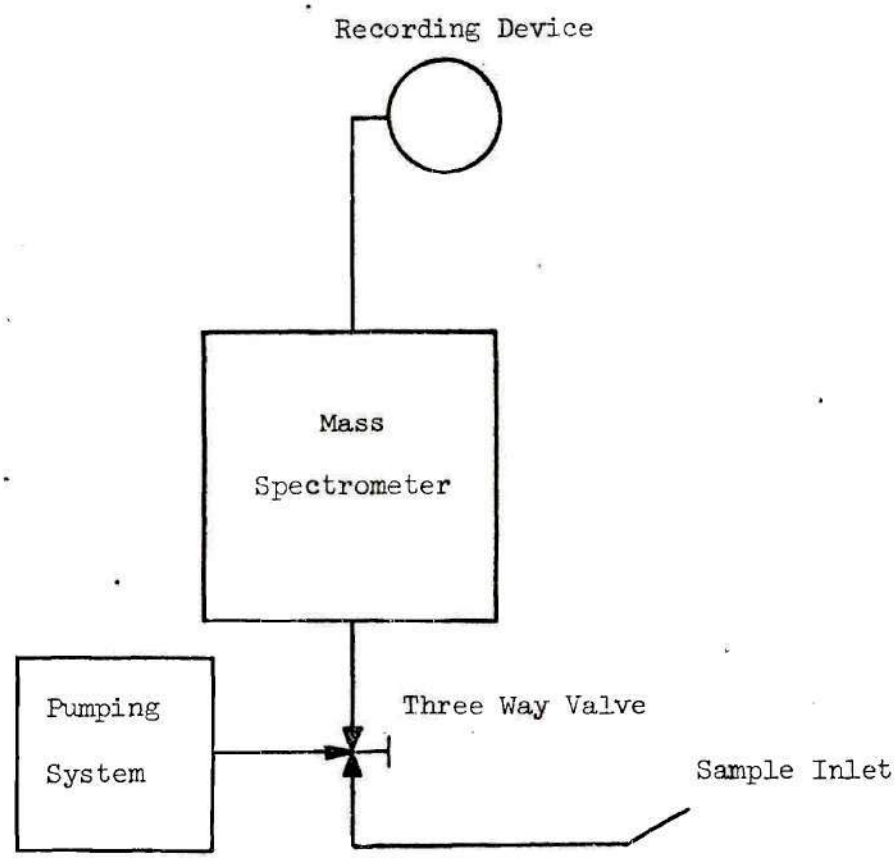

Figure 4. Respiratory Mass Spectrometer System.

the TGA can be switched manually between any four preset mass to charge ratios, or will measure simultaneously any two desired mass to charge ratios by rapid electronic switching between two channels.

The Sampling System

One of the most critical parts of the respiratory mass spectrometer is the sampling system. The sampling system must deliver to the mass spectrometer a continuous and representative sample. For this application, fine capillary tubing has been found to be most satisfactory (21). This tubing gives reasonably low flow rates, small response times, minimum mixing down the tube, and the downstream pressure is easily maintained at the low pressures required to operate the mass spectrometer (21).

When discussing the response time characteristics of the sampling system, two distinct time intervals are commonly specified. Referring to Figure 5, the time required for the first detection of a change in the sampled gas is referred to as the lag time (TL). The time from first detection until the reading is 90 percent of the full scale deflection is referred to as the rise time (TR). In the development of a sampling system, it is desirable to have both times minimized. A small rise time is required to assure that accurate and representative readings are being taken on the rapidly changing gases. While hyperventilating at a rate of 40 breaths per minute (a rate three to four times that found in normal breathing, and one and one-third times that anticipated for the present study), one breath is taken every one and one-half seconds. During this time, there are three segments of interest; inhalation, exhalation, and the time between the inhalation

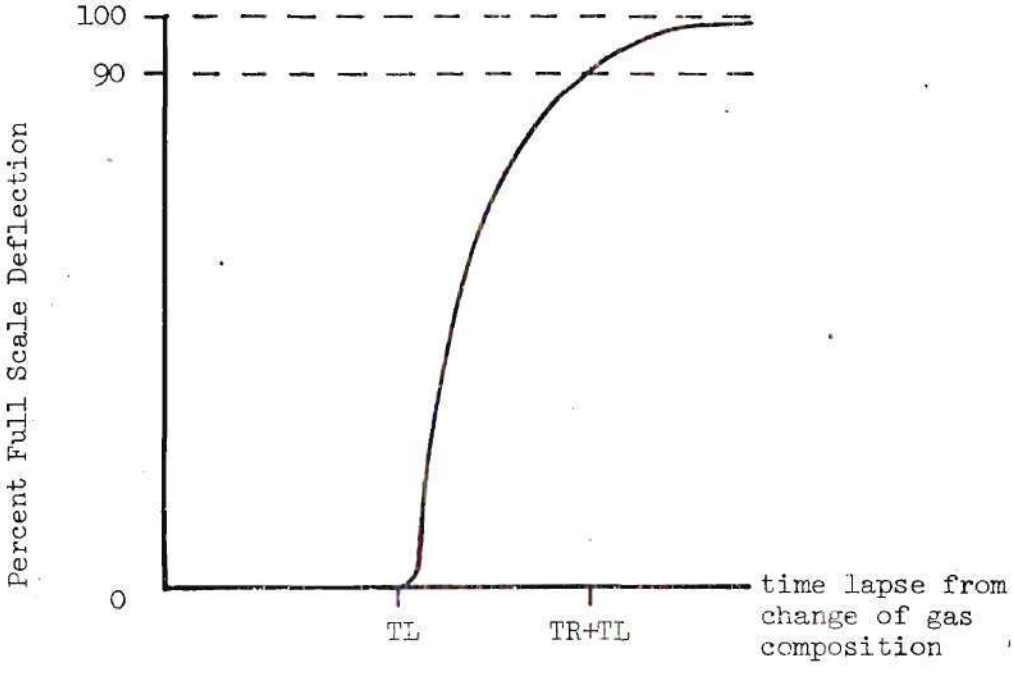

Figure 5. Response Curve Definitions.

and exhalation. If a single breath is subdivided into six periods, the time required for one segment to occur is 250 milliseconds (msec). In order to accurately predict what is happening in the segment, sampling theory (23) dictates that two data points would have to be measured, or that the rise time must be 125 msec. This estimation agrees with the 100 msec rise time which Fowler (14) sets a requirement for accurate measurement during respiratory analysis.

In modeling the gas flow of a sampling system, Hagen-Poisuille flow can be assumed to exist down the capillary (21,24). Appendix I presents the steps and assumptions used in acquiring the following equations. Referring to Figure 6 for the symbols, the mass flow rate, W, can be written as (see Appendix I),

$$W = \frac{kR^4}{\mu L} (P_1^2 - P_2^2) \qquad (1)$$

where k is a constant depending on the units used.

The lag time can be written as,

$$TL = \frac{16L^{\frac{3}{2}}}{3\sqrt{\frac{W}{k}}} \qquad (2)$$

It is also shown in Appendix I, that, under the assumption of no mixing down the tube, the rise time is 10 times the lag time.

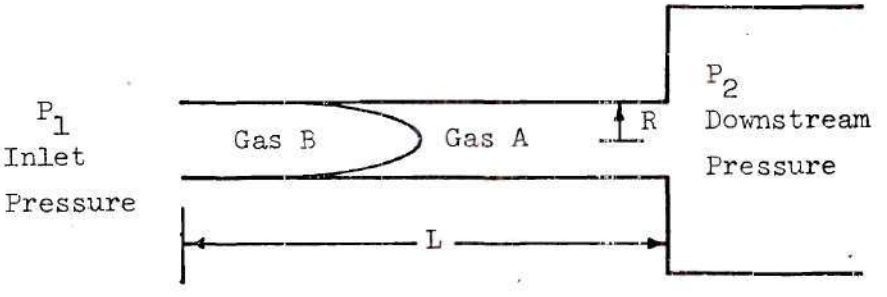

Figure 6. Analytical Model for Determination of Response Times.

Under the conditions of mixing (25,26,27), Gas B moves radially into Gas A, and Gas A moves radially into Gas B, thus blunting the shape of the concentration profile and reducing the rise time (20). Equation (2) still holds for the lag time, but now the rise time is different. Using the results of Taylor (26,27) the rise time can now be written as (see Appendix I)

$$TR = TL \left(\frac{L_T}{L}\right)^{\frac{3}{2}} \qquad (3)$$

where L_T, the transition zone length, is the distance between the 0 and 90 percent planes of the concentration profile as determined by Taylor.

Experimental determination of the lag and rise times is accomplished by inserting a probe on the end of the sample line into a stream of nitrogen and recording the oxygen partial pressure on one channel of a two channel storage oscilloscope (see Figure 7). The test probe is connected by alligator clips into a circuit with an applied three volt potential. When the test probe is withdrawn vigorously from the nitrogen stream, two things happen simultaneously. The alligator slip in the tube is pulled off the probe breaking the circuit, and the probe is exposed to the oxygen in the atmosphere. Figure 8 shows a sample trace obtained by this method. When the circuit is broken, a three volt drop is shown on the scope, and at some time later, the oxygen peak is recorded. Thus the time lapse before detection as well as the rise time can be measured.

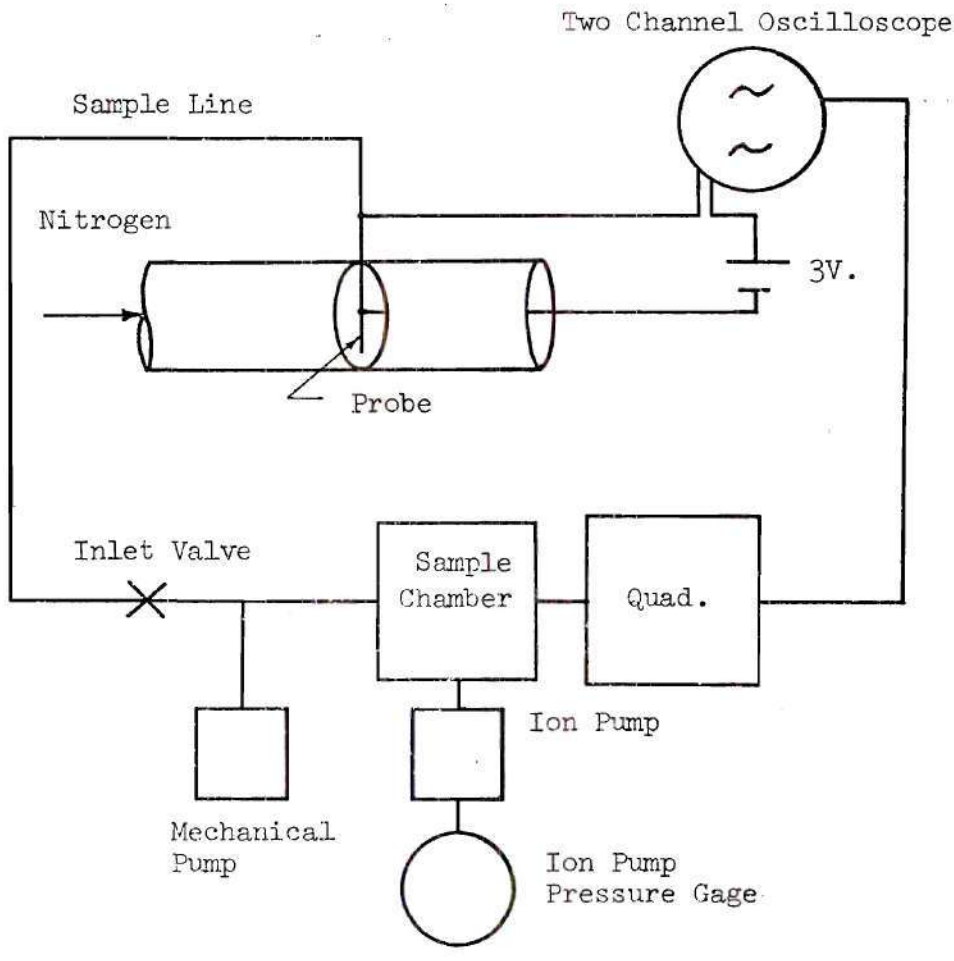

Figure 7. Experimental Circuit for Response Time Determination.

Figure 8. Sample Experimental Trace for Determination of Response Times.

Table 1 shows the data gathered experimentally and the corresponding times determined from equations (2) and (3) for lag time, and rise time at various radii and lengths of the sample line. The experimental data shows very little change in lag time with radius for a given length while the analytically determined lag times vary with length and radius. Both indicate little change of rise time with length or radius. While the corresponding lag times found experimentally and analytically were, in general, of the same order of magnitude, there was a considerable error in the rise time determination.

The difference between the experimental and analytical determination of the response times could be due to several factors such as dead space and resistance in the system which was not accounted for in the analytical model. The assumptions used in acquiring equations (2) and (3) do not always meet the conditions faced in the sampling system. For example the ion pump must be protected from pressures above 10^{-4} mmHg. This means that the inlet valve must be adjusted to keep the mass flow rate to the ion pump within a reasonable range. With increasing tube diameter or decreasing tube length, the mass flow to the quadrupole and ion pump increases. It was desired that the conditions of the experimental determination of the response times be the same as encountered during testing. Therefore, during experimental determination of the response time, the mass flow rate to the vacuum pump was kept constant by regulation of the inlet valve. The advantage of increasing the mass and volume flows with increasing tube diameters is that the response times decrease (see equation (2)). This advantage, however, must be weighed

Table 1. Response Times in Relation to Tube Diameter and Length.

Diameter (ID) in inches	Length in inches	Analytical Lag Time in msec.	Analytical Rise Time in msec.	Experimental Lag Time in msec.	Experimental Rise Time in msec.
.018	72	92	2	130	20
.022	72	62	2	86	18
.027	72	41	2	80	18
.034	72	26	2	80	16
.018	60	64	2	-	-
.022	60	43	2	66	18
.027	60	28	2	66	18
.034	60	18	2	68	16
.018	48	41	2	36	20
.022	48	27	2	46	14
.027	48	18	2	48	14
.034	48	12	2	52	16
.018	36	23	1	44	20
.022	36	15	1	36	16
.027	36	10	1	38	14
.034	36	6	1	42	16
.018	24	10	1	24	18
.022	24	9	1	26	14
.027	24	5	1	28	16
.034	24	3	1	30	20

against the disadvantage of wear to the ion pump. Therefore, by using the inlet valve to reduce the mass flow to the ion pump, the effect of tube diameter on the response times was lost.

The sampling system used in the present study consisted of two lengths of .016 diameter tubing connected by a small valve. The added dead space and resistance of the valve resulted in an experimentally determined rise time of 80 msec. This rise time was less than the 100 msec time desired for the purposes of these tests.

Calibration

The sampling system used in this study consisted of a capillary tubing from the quadrupole inlet to a modified commercial valve. This valve allowed rapid switching between a capillary tube to a calibration gas and a capillary tube to the sampled stream. One of the requirements for accurate calibration of the TGA is that the pressure drop existing down the line from the valve to the calibration gas and the line from the valve to the sampled stream must be the same.

This arrangement proved satisfactory for sampling dry gas mixtures. However, in breath by breath analysis the sampled gas is not always dry. The exhaled gas mixtures sampled were saturated with water vapor at body temperature and as the exhaled gases traveled down the line, water vapor condensed on the walls of the tubing, creating conditions which were not duplicated in the calibration line. In order to overcome this water vapor problem, a calibration procedure was evolved as discussed below.

The TGA was used to monitor the water vapor present in the

sampled gas mixture, and the probe was inserted into a stream of air saturated with water vapor at body temperature. The TGA showed a partial pressure of 47 mmHg of water vapor in the gas. The probe was then withdrawn from the wet gas mixture and inserted into a stream of dry gas. It was several minutes before the indicated water vapor dropped from its level of 47 mmHg, indicating that the water vapor remained in the system for several minutes before the dry air could dry out the system.

Under the conditions of sampling respired gases, the inspired air contained water vapor as determined by the relative humidity, while the expired gas contained 47 mmHg of water vapor. However, after several minutes of sampling respired gases, the water vapor from the expired gas saturated the system, and the indicated water vapor present in the system was 47 mmHg.

The absence of water vapor on the walls of the calibration line resulted in the calibration line readings being higher than the sample line readings when reading the same gas mixture. Therefore, the FIO_2 and $FICO_2$ values, which were always known, were used as calibration points for data correction.

The problem of water vapor condensing in the lines can be eliminated by using small bore metal tubing and heating it above body temperature. Under these conditions, however, the water vapor in the sample chamber of the quadrupole becomes a problem. The water vapor tends to linger in the sample chamber thus interfering with the reading of the desired gases (22).

For the purpose of this study, it was decided to allow the lines

and sample chamber to saturate with the water vapor, and use the inspired values for calibration. First the inspired gas partial pressures were determined by taking into account the partial pressure of water vapor in the inspired air. This partial pressure of water vapor was subtracted from the barometric pressure to give the total pressure of the dry inspired gases. From this value, the partial pressures of the inspired gases were determined. The expired gases, however, were saturated with water vapor at body temperature, and contained 47 mmHg of water vapor. Therefore, the total pressure of the dry expired gases was the difference between the barometric pressure and the water vapor partial pressure in the expired gas mixture. As the TGA readings had been corrected to dry inspired readings, the expired readings were multiplied by the ratio of the total dry inspired pressure to the total dry expired pressure to correct the readings.

The Inspiratory Control Unit

For testing it was desired to control the end expired carbon dioxide and oxygen partial pressures. The partial pressure of oxygen can be controlled by regulation of the FIO_2. The carbon dioxide, however, is produced within the body, and it was not possible to lower the $PACO_2$ below its normal value of about 42 mmHg by inspired gas regulation during regular breathing. In order to vary the end expired carbon dioxide partial pressure, it was necessary to have the subject hyperventilate, reducing the end expired carbon dioxide partial pressure, and add carbon dioxide to the inspired gas. To accomplish this, the Inspiratory Control Unit, ICU, was built. The ICU is shown graphically in Figure 9.

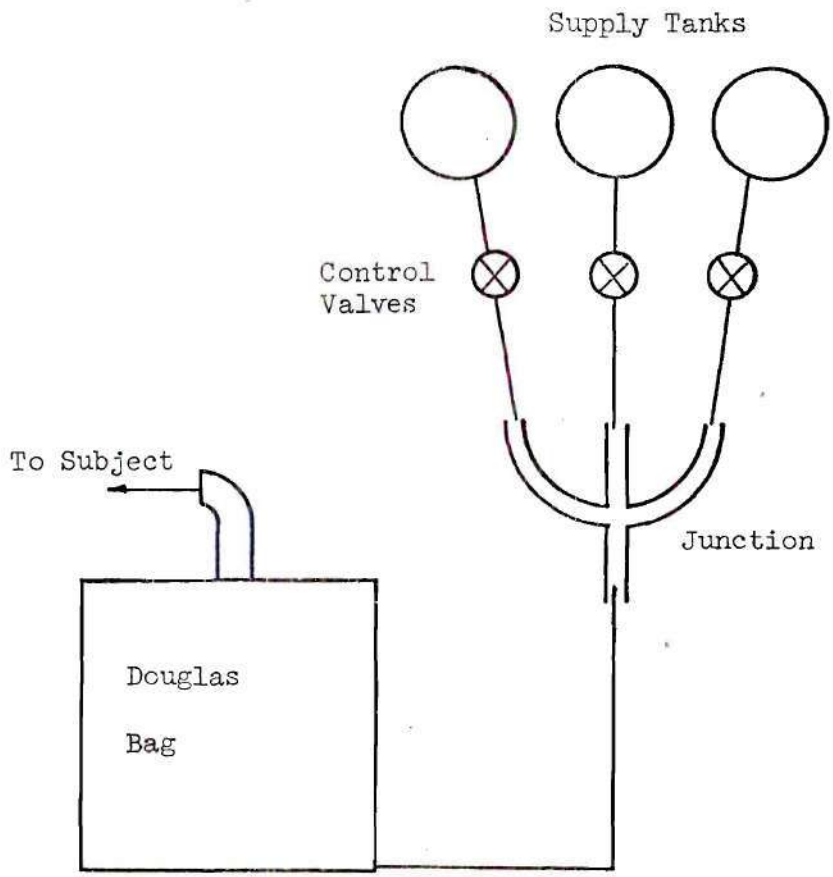

Figure 9. Inspiratory Control Unit.

The gas flows from the tanks, through flowmeters, and into the junction where the gases are combined into one stream. The combined gases then flow into the bottom of the Douglas Bag, which acts as a reservoir, and mixes with the gas already in the bag. The mixed gas which flows to the subject is drawn from the top of the bag.

Other Equipment

The complete experimental circuit is shown in Figure 10. The ICU delivered a gas of any mixture to the subject through a one way valve and a pneumotachograph. The TGA sample probe was inserted through the mouthpiece into the stream of respired gases. A pressure transducer, which sensed the pressure drop across the resistance in the pneumotachograph, sent a flow rate signal to the Sanborn four channel recorder where the flow rate was integrated to give the tidal volume. Both values were continuously recorded on the Sanborn.

Other equipment used but not shown in the Figure were an IL313 Blood Gas Analyzer, and a metronome used to pace the subjects' breathing rate. The testing was performed at Grady Memorial Hospital in Atlanta, Georgia, and the blood gas analysis was done by a pulmonary technician at the hospital.

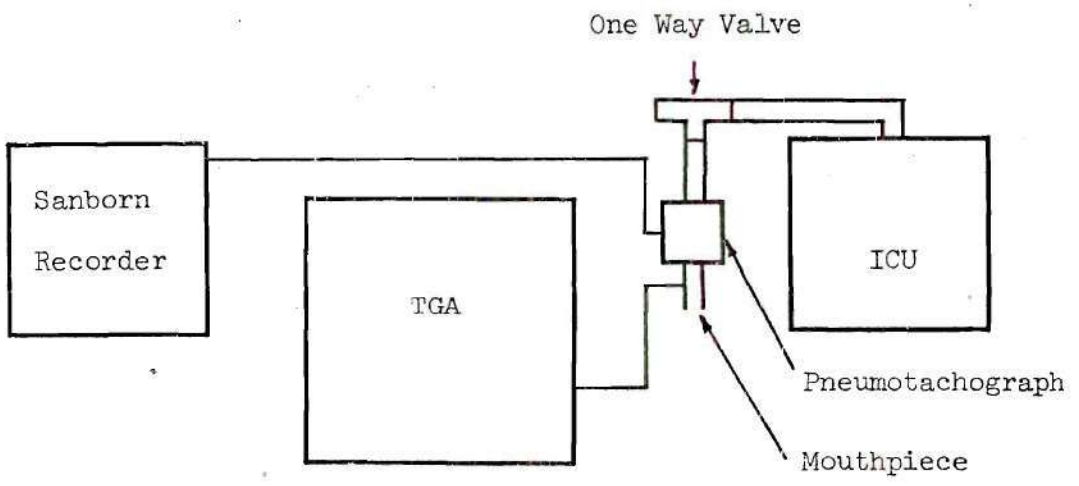

Figure 10. Testing System.

CHAPTER III

PROCEDURE

Preparation

The testing of seven subjects was carried out over a period of several months at Grady Hospital under the supervision of Dr. Roland Ingram from Emory University. The subject's arm was given a local anesthetic, and a cannula was inserted into the radial artery for blood withdrawal during testing.

Testing

The testing was conducted in two segments. The Series One testing was a procedure similar to that carried out by Pichotka (13) in the paper previously mentioned. The subject began by sitting and breathing normally on room air through the mouthpiece (i.e., the ICU was not in the system), becoming accustomed to breathing on the system. The subject's acclimation to the system was determined by the steadiness of the end expired partial pressures as recorded by the TGA. Once this steady state of end expired gases was noted, two minutes were allowed to let the subject's system come to steady state before blood was taken. After the two minute period the first blood sample was taken in a heparinized syringe, and at the time of blood withdrawal the corresponding end expired values on the TGA trace were noted. The subject was then instructed to begin mild hyperventilation until the end expired carbon dioxide value had dropped by approximately 5 mmHg.

Once the end expired partial pressures had reached steady state values, the subject was coached for two minutes to maintain a constant tidal volume and breathing rate before blood was taken. After this two minute period, blood was taken, and again the corresponding end expired partial pressures were noted on the TGA trace.

The process was repeated until the subject's end expired carbon dioxide partial pressure was reduced to approximately 15 mmHg, making sure that during the two minute periods the TGA readings on end expired values remained reasonably constant. In the instances that the TGA readings showed changing conditions in the end expired values, the subject was coached back to the desired level, and the two minute period started over again.

After the subject had reached full hyperventilation and the blood had been withdrawn, data was taken during the post-hyperventilation period. For these data, the subject was instructed to resume normal breathing through the mouthpiece. Blood samples were taken at 2 1/2, 5, and 8 minutes after normal breathing had resumed and the corresponding end expired partial pressures were marked on the TGA output.

For Series Two tests the ICU was attached to a one way valve which was in turn attached to the pneumotachograph. The subject began by sitting and hyperventilating on dry air delivered to the mouthpiece by the ICU. The ventilation rate was the same as that found necessary to bring the end expired carbon dioxide partial pressure to approximately 15 mmHg in the Series One testing. The subject's breathing rate was preset on a metronome to which the subject paced

his breathing during the entire test. The subject's tidal volume was monitored on the Sanborn recorder, and this reading was used to coach the subject to maintain a constant tidal volume throughout the entire test. After the subject's end expired partial pressures reached steady state, two minutes were again allowed before blood was withdrawn. Again, as the blood was withdrawn, the corresponding end expired partial pressures were marked on the TGA trace. At this point, enough carbon dioxide was added to the inspired gas mixture to raise the end expired partial pressure of carbon dioxide by approximately 5 mmHg, and the same procedure was repeated.

This process was continued until the subject's end expired carbon dioxide partial pressure had been varied over the same range as in the Series One testing, which was from approximately 15 to 45 mmHg. Again, if the TGA readings showed changing conditions in the end expired values, the subject was coached back to the desired level, and the two minute period started over again.

During the Series Two testing, no attempt was made to control the PAO_2 (assumed to be the end expired partial pressure of oxygen) as the FIO_2 and PAO_2 varied little (3.7 mmHg maximum average variation of PAO_2 within individual data, and an average deviation in PAO_2 of 2.2 mmHg from subject to subject) during carbon dioxide addition. The conditions under which the Series Two tests were made can thus be described as varying $PACO_2$ (assumed to be the end expired partial pressure of carbon dioxide) with constant ventilation (tidal volume times breathing rate) and PAO_2, while the Series One test conditions were varying $PACO_2$, PAO_2, and ventilation.

CHAPTER IV

RESULTS AND DISCUSSION

Series One

The Series One test data on six normal subjects (one repeated) between the ages of 24 and 32 is given in Appendix II. Figures 11 and 12 show the variation of the $AaDO_2$ with the $PACO_2$ and PAO_2, respectively, as found in the Series One tests. Although the $AaDO_2$ measurements in the present study were consistantly smaller in magnitude than those found by Pichotka (13) in the same ranges of $PACO_2$ and PAO_2, the trends shown in the Figures are comparable with the commonly observed trends of increasing $AaDO_2$ with decreasing $PACO_2$ and increasing PAO_2 found by several investigators (2,7,8,9,12,13) including Pichotka. There was, however, a significant difference in the post-hyperventilation data. Pichotka concluded that the dependence of $AaDO_2$ on $PACO_2$ was stronger than the dependence on PAO_2 on the basis that for the post-hyperventilation data, the $AaDO_2$-$PACO_2$ relationship was consistant with the relationship shown during hyperventilation while the post-hyperventilation $AaDO_2$-PAO_2 relationship was not consistant with the $AaDO_2$-PAO_2 hyperventilation relationship.

Table 2 gives the results of a linear regression performed on the data for the $AaDO_2$ versus $PACO_2$ and PAO_2 without and with the post-hyperventilation data. From Table 2, the standard deviation and correlation coefficient (R) in the $AaDO_2$-$PACO_2$ relationship are

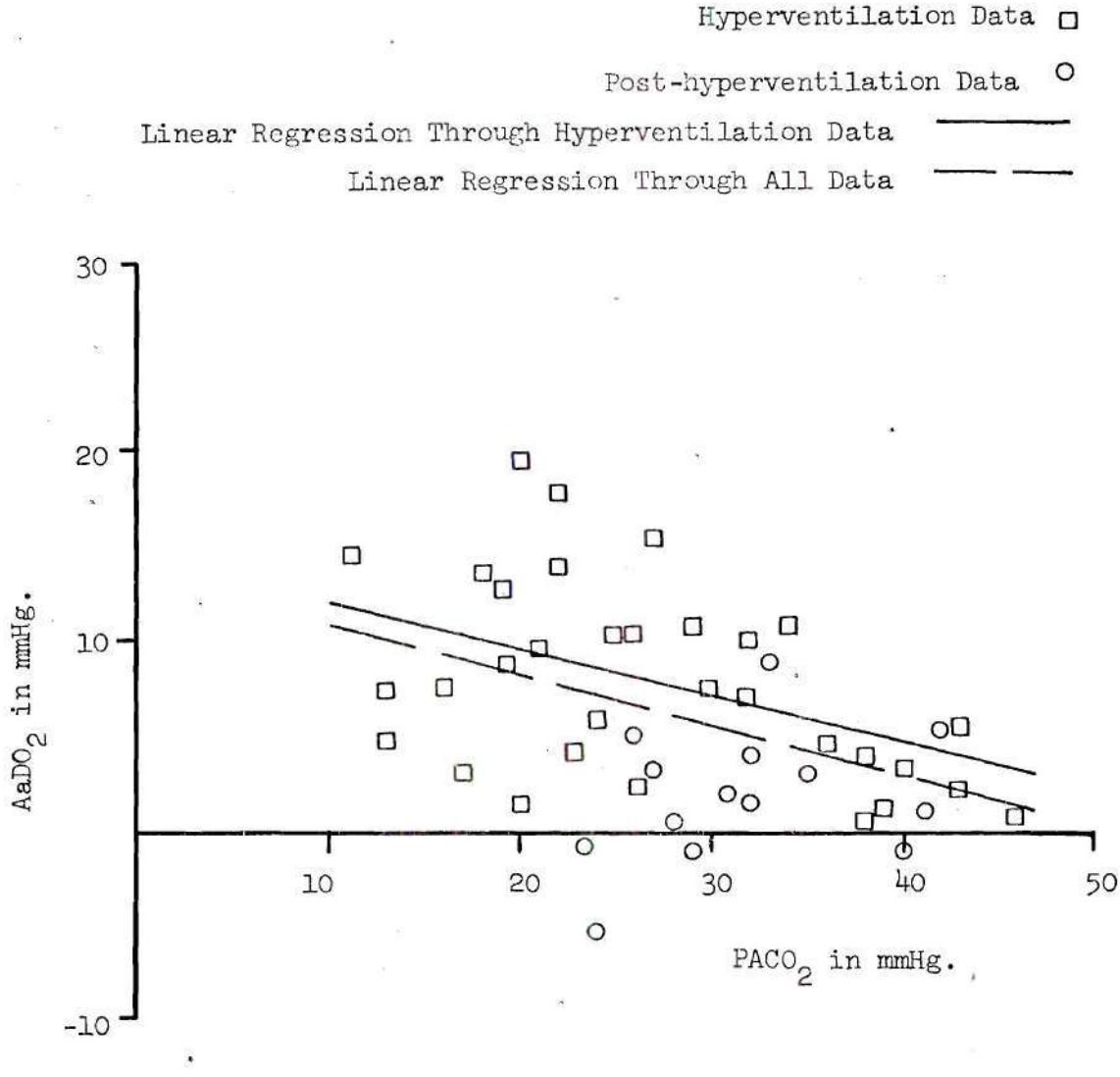

Figure 11. $AaDO_2$ Versus $PACO_2$ in Series One Tests.

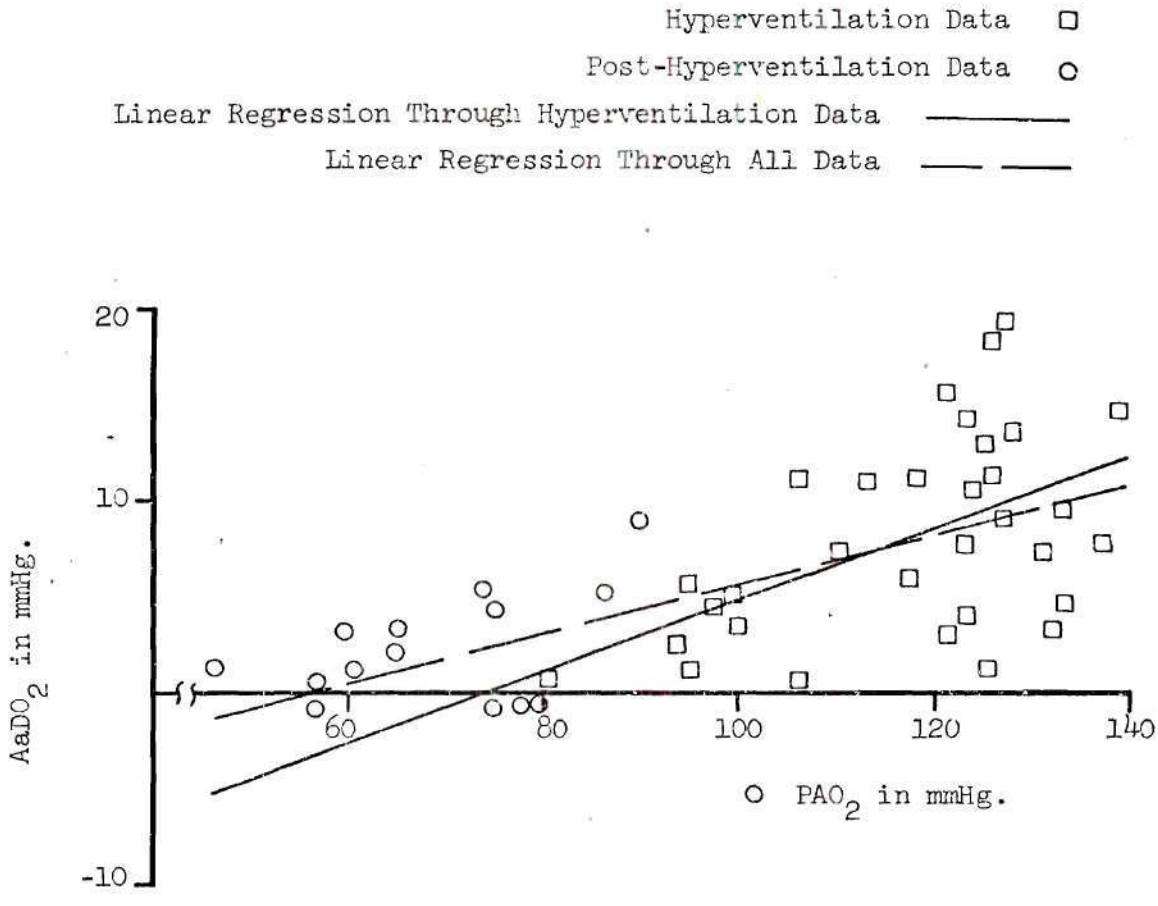

Figure 12. $AaDO_2$ Versus PAO_2 in Series One Tests.

Table 2. Results of a Simple Linear Regression.

Series	$AaDO_2$ vs	Slope	Intercept	Standard Deviation	R,(P)***
1(32)*	$PACO_2$	-.25	14.75	4.7	-.46,(<.001)
1(47)	$PACO_2$**	-.26	13.65	5.0	-.43,(<.002)
1(32)	PAO_2	.18	-12.79	4.6	.51,(<.002)
1(47)	PAO_2**	.13	-7.3	4.3	.62,(<<.001)
2(32)	$PACO_2$	-.09	13.64	4.5	-.18,(.2-.5)

* The number enclosed in parenthesis represents the number of data points taken.

** This relationship includes the post-hyperventilation data taken.

*** R is the correlation coefficient which (as defined in Lectures on Biostatistics (30)) gives the degree of correlation between the variables - ±1.0 representing a perfect correlation while 0 indicates no correlation. P is the probability of no correlation between the variables, a value greater than .05 leaving reasonable doubt that the results actually are conclusive that a correlation exists.

comparable with those noted for the $AaDO_2$-PAO_2 relationship. Also, the value of the probability P (30) indicates that there is a small probability that no correlation of variables exists in either case.

When the post-hyperventilation data is added to the regression procedure, the $AaDO_2$-$PACO_2$ relationship becomes weaker as the standard deviation increases and the correlation coefficient becomes smaller. This would indicate that the $PACO_2$ correlates better with the $AaDO_2$ without the post-hyperventilation data. However, when the post-hyperventilation data is added to the regression procedure for the $AaDO_2$-PAO_2, the standard deviation decreases and the correlation coefficient increases, indicating an even better fit to a straight line when the post-hyperventilation data is added. In both cases, the P value indicates that a correlation between the variables exists.

Therefore, there are two results which lead to the conclusion that the $AaDO_2$ correlates better with the PAO_2 during the Series One procedure. First, the correlation coefficients in Table 2 indicate that the $AaDO_2$-PAO_2 relationships were stronger than the $AaDO_2$-$PACO_2$ relationships. Secondly, the post-hyperventilation data correlated better with the $AaDO_2$-PAO_2 relationship than with the $AaDO_2$-$PACO_2$ relationship.

These results are in conflict with those found by Pichotka (13). In fact, the $AaDO_2$-$PACO_2$ relationship was reported to be much stronger than the $AaDO_2$-PAO_2 relationship in Pichotka's tests (based on the fit of the post-hyperventilation data) and Pichotka inferred that the $PACO_2$ was the controlling factor in the magnitude of the $AaDO_2$.

One of the differences noted between Pichotka's procedure (13) and that of the Series One tests of the present study was the method of blood gas analysis. As stated previously, the blood gas partial pressures in Pichotka's tests were taken from a hyperamized earlobe by polarographic methods. This involves oxygen diffusing from the blood, through the earlobe, and through the membrane of the measuring device. The signal transmitted is proportional to the number of oxygen molecules crossing the membrane. During hypocapnia, which is induced by the hyperventilation, vasoconstriction occurs in the small capillaries of the skin (29). This means that less blood is passing through the earlobe, and even if the PAO_2 remains unchanged, there is less oxygen to diffuse through the membrane simply because there is less blood passing through the capillaries. This would mean that the blood gas measurements on oxygen made by Pichotka could have been low during hyperventilation.

Series Two

The Series Two test data on the same group with the addition of one subject is presented in Appendix II. Figure 13 represents the trend displayed between the $AaDO_2$ and $PACO_2$ during the Series Two tests with constant hyperventilation over the same range of $PACO_2$ as that of the Series One tests.

Table 2 contains the results of the regression performed on the $AaDO_2$ versus $PACO_2$ in the Series Two tests. The results indicate that the slope is near zero (-.09) and the correlation coefficient is low (-.18), or that the $AaDO_2$ does not vary with $PACO_2$ during constant

ventilation and PAO_2 at values of FIO_2 near that of air. The P value (between .2 and .5) also leads to the conclusion that the $AaDO_2$ shows no correlation with the $PACO_2$ under the conditions of Series Two testing.

Normalization

The scatter in the data shown in Figures 11, 12, and 13 could be partially attributed to the physiological differences from subject to subject. In an attempt to reduce the scatter, a normalization was performed on each subject's set of data. The average $AaDO_2$ was determined for each subject and used to normalize the data about one by dividing each subject's $AaDO_2$ by his average (giving the $\overline{AaDO_2}$).

Figures 14, 15, and 16 show the results of the normalization procedure for $\overline{AaDO_2}$ versus $PACO_2$ and PAO_2 from Series One, and $\overline{AaDO_2}$ versus $PACO_2$ in Series Two respectively. Table 3 gives the results of a linear regression performed on the normalized data. The correlation coefficients all increase from the corresponding values in Table 2, showing a closer fit to the determined line. The $\overline{AaDO_2}$ demonstrates the same statistically stronger relationship with PAO_2 as did the $AaDO_2$. When the post-hyperventilation data is included in the linear regression for $\overline{AaDO_2}$ versus $PACO_2$, the standard deviation increased while the correlation coefficient decreased from the values determined without the post-hyperventilation data. The same changes are also noted when the post-hyperventilation data is added to the linear regression for $\overline{AaDO_2}$ versus PAO_2. However, the standard deviation and correlation coefficient indicate that the $\overline{AaDO_2}$-PAO_2 relationship is stronger than the $\overline{AaDO_2}$-$PACO_2$ relationship.

The linear regression on the normalized Series Two data gives

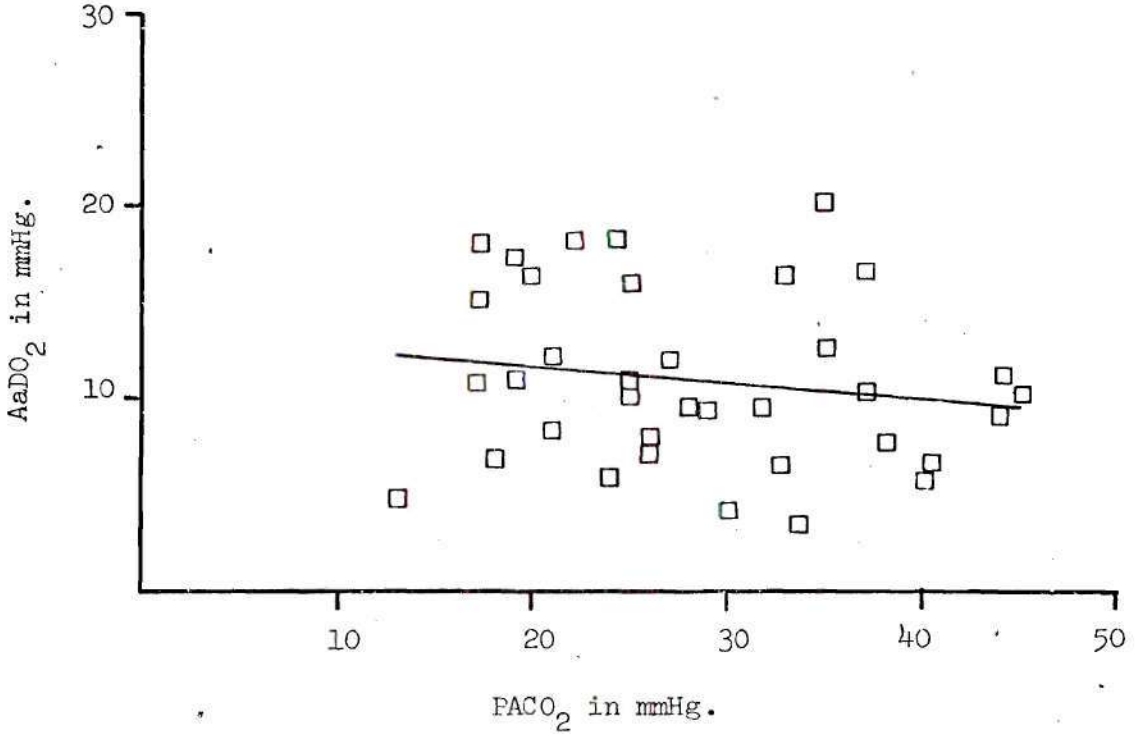

Figure 13. $AaDO_2$ Versus $PACO_2$ in Series Two Tests.

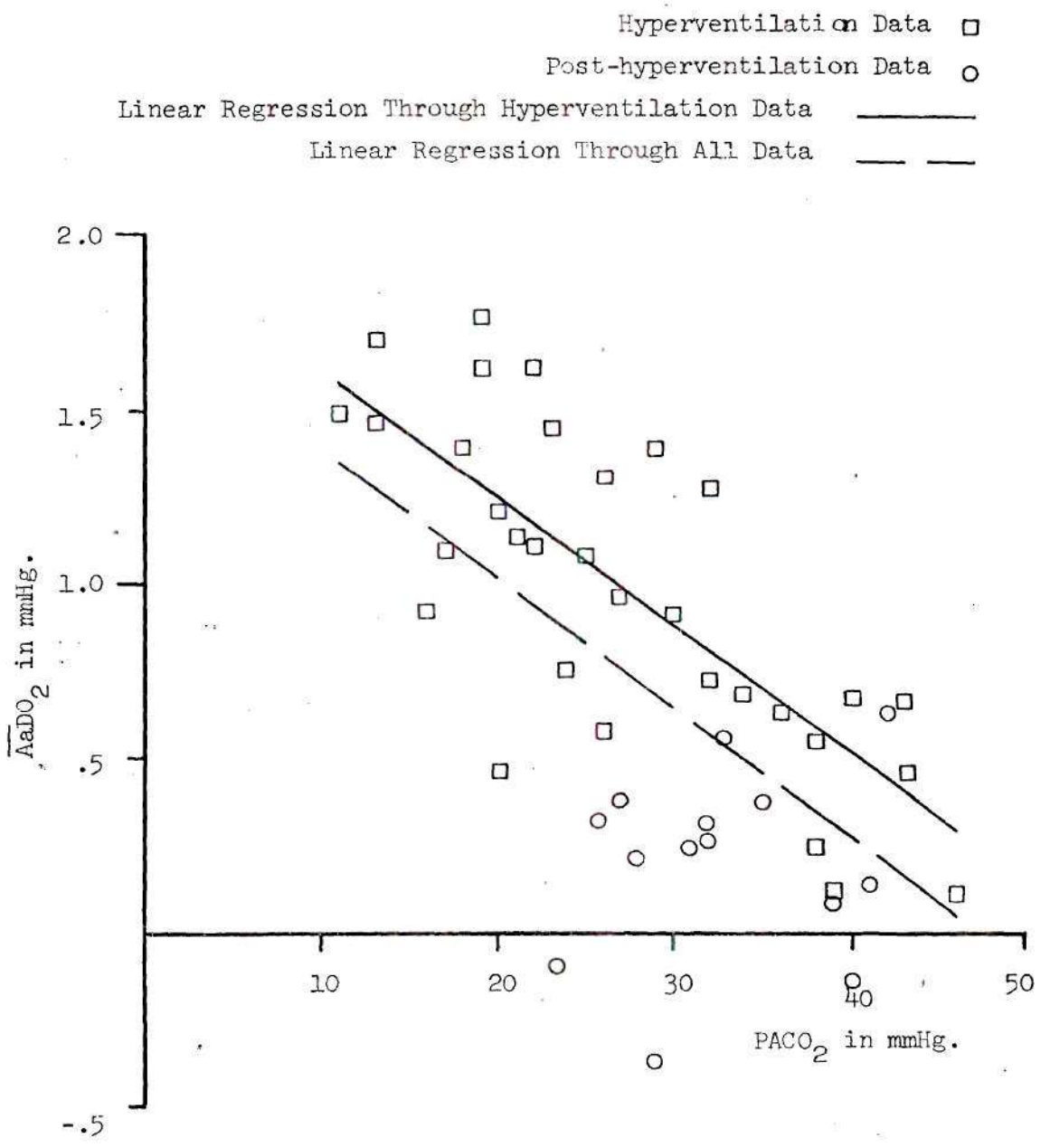

Figure 14. $\overline{AaDO_2}$ Versus $PACO_2$ in Series One Tests.

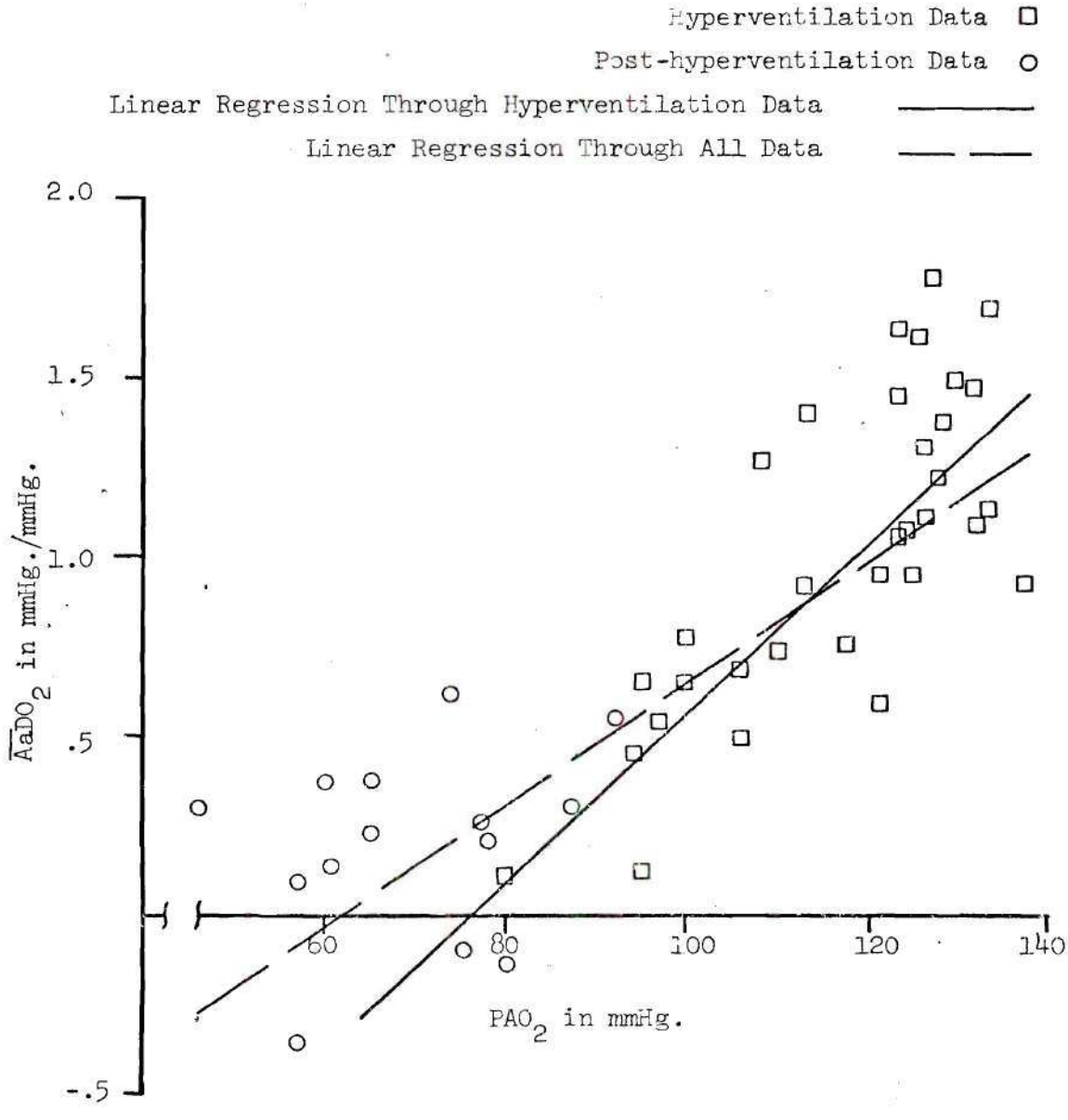

Figure 15. $\overline{AaDO_2}$ Versus PAO_2 in Series One Tests.

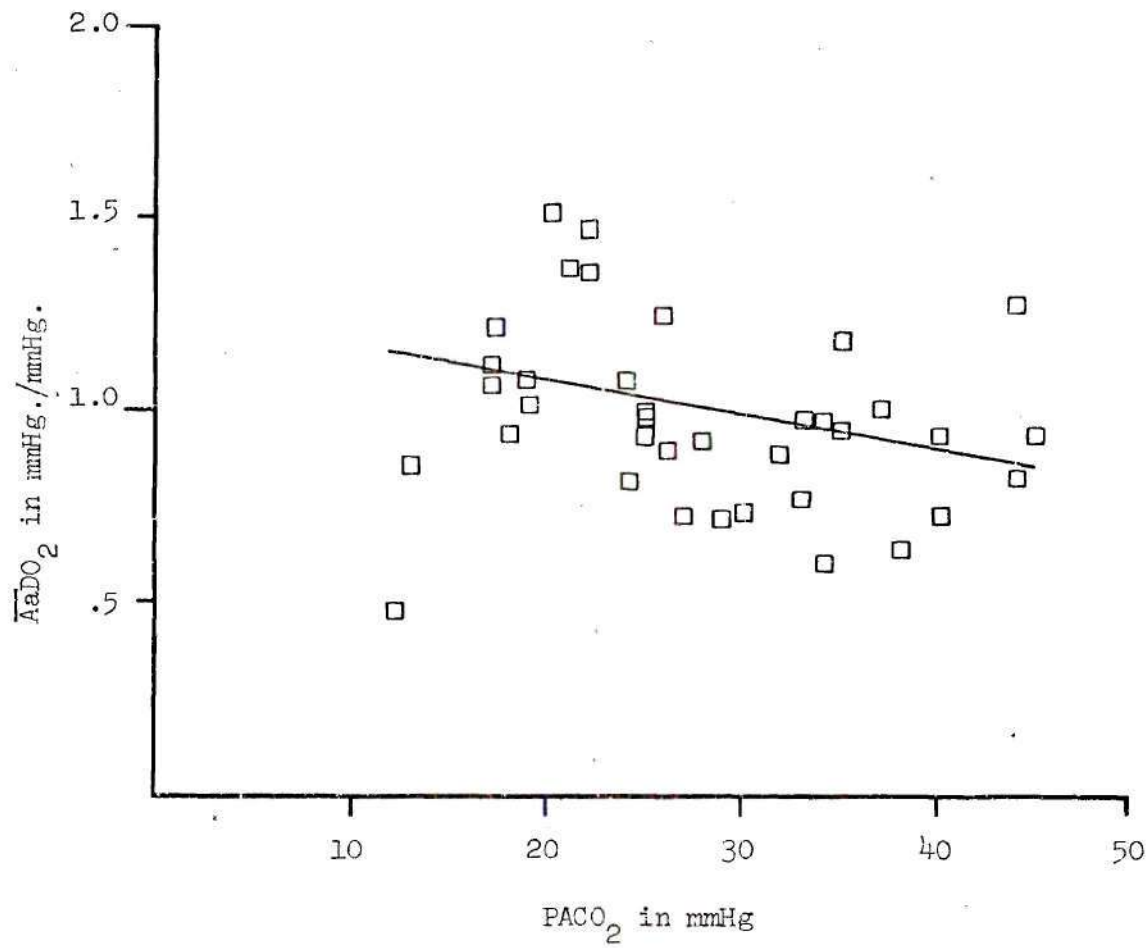

Figure 16. $\overline{AaDO_2}$ Versus $PACO_2$ in Series Two Tests.

Table 3. Results of a Simple Linear Regression on Normalized Data

Series	$\overline{AaDO_2}$ vs	Slope	Intercept	Standard Deviation	R,(P)***
1(32)*	$PACO_2$	-.0369	1.988	.313	-.758,(<<.001)
1(47)	$PACO_2$**	-.0368	1.754	.586	-.496,(<<.001)
1(32)	PAO_2	.0237	-1.789	.320	.745,(<<.001)
1(47)	PAO_2**	.0172	-1.0661	.499	.673,(<<.001)
2(32)	$PACO_2$	.0089	1.252	.212	-.348,(.02-.05)

* See note on Table 2.

** The linear regression was performed on the data including the post-hyperventilation data points. The post-hyperventilation data was not included in the averaging to find the average $AaDO_2$.

*** See note on Table 2.

a near zero slope. The correlation coefficient is also lower than the corresponding correlation coefficient from the Series One test (-.348 in Series Two versus -.758 in Series One). The result is essentially a horizontal line indicating that the $\overline{AaDO_2}$, and thus the $AaDO_2$, is independent of the $PACO_2$.

A Hypothetical Model

The series Two test results indicate that, contrary to Pichotka's (13) conclusions, the $AaDO_2$ is independent of $PACO_2$. Therefore, some other factor must be influencing the $AaDO_2$. In the six subjects studied in the Series One tests, all were young (24-32 years old) healthy subjects. There was no reason to believe that either the diffusion limitations would be great, or that there was a large $\dot{V}/\dot{Q}$ in any of the subjects. In Figure 3, it was noted that the $AaDO_2$ due to the $\dot{V}/\dot{Q}$ imbalance was fairly low and constant. It would seem that neither of these factors could produce the magnitude changes of $AaDO_2$ with PAO_2 as noted in Figure 12. Shunting, however, could cause the changes noted, as every person has some degree of shunting (2 percent and less being normal (4)).

In order to model shunting, the transportation of oxygen in blood must be considered. Oxygen is transported in the blood by two means; chemically forming a weak bond with hemoglobin (forming oxyhemoglobin), and physically dissolved in the blood. In both cases, the amount of oxygen in the blood depends on the partial pressure of oxygen to which the blood is exposed. While the amount of oxygen dissolved in the blood is linearly related to the oxygen partial pressure, the amount of oxygen combining with the hemoglobin is related to the

oxygen partial pressure by the hemoglobin dissociation curve.

In order to determine the effect of shunting on the $AaDO_2$ for a given PAO_2 and venous partial pressure of oxygen (PvO_2), the content of the blood passing the alveoli is added to the oxygen content of the blood which bypasses the alveoli in proportion to their respective blood flows. An iterative procedure is then carried out to determine what PaO_2 yields the same oxygen content as the combined content found previously. The difference between the PAO_2 and PaO_2 gives the $AaDO_2$ due to the shunt at that particular PAO_2, shunt size, and PvO_2.

To accomplish this procedure, a computer program was written in which the oxyhemoglobin dissociation curve (assuming a pH of 7.4 and a temperature of $38^{\circ}C$) was approximated by a double exponential (31) relating the partial pressure of oxygen present to the volume of oxygen combined with hemoglobin in 100 milliliters of blood. The volume of oxygen dissolved in 100 milliliters of blood was determined by a linear relationship where the dissolved oxygen was related to the partial pressure of oxygen present by a constant (.0003026) (32). The computer program and the results for shunt fractions of 2, 5, and 10 percent are presented in Appendix III.

Figure 17 shows the relationship found by computer simulation for $AaDO_2$ versus PAO_2 and the percent of the total blood flow shunted. The Figure shows that the $AaDO_2$ increases with increasing PAO_2 until at some value of PAO_2 the $AaDO_2$ reaches a plateau. Also, the $AaDO_2$ at any given PAO_2 increases with shunt size.

The variation of pH during hyperventilation does have an effect

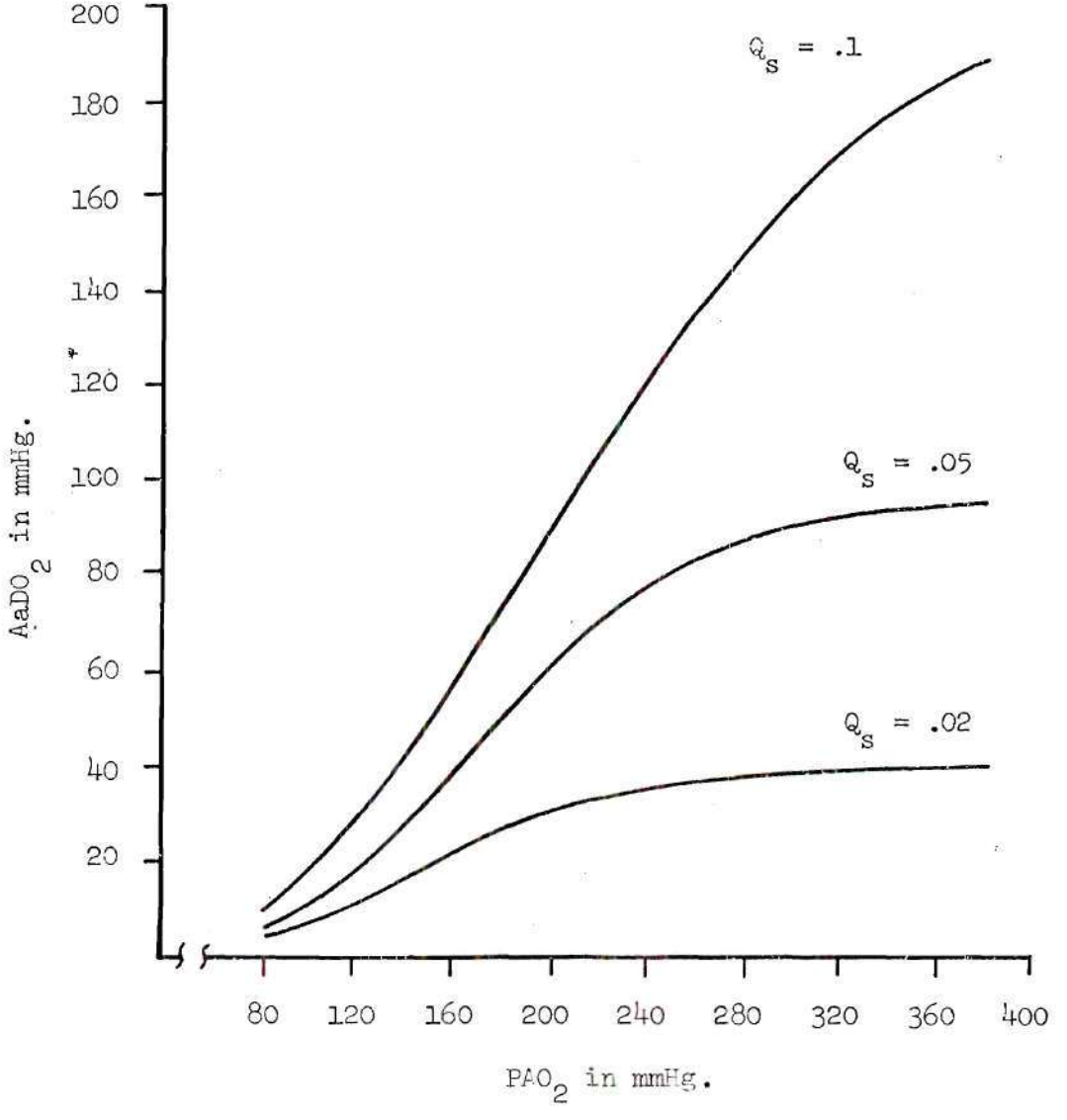

Figure 17. Effects of Shunting on $AaDO_2$ at Various Levels Of PAO_2.

on the shape of the shunt curves generated. With decreasing $PACO_2$, the results of using a pH of 7.4 to determine the PaO_2 leads to an overestimation of the PaO_2 and thus an underestimation of the $AaDO_2$. Thus, in the hyperventilation and post-hyperventilation region of Figure 17 (above 100 mHg and below 90 mmHg approximately for the PAO_2 respectively) the $AaDO_2$ would be expected to be higher than that predicted by the shunt line. Consideration of the changing pH was not included in the shunt model as it would be impractical to consider the variations of pH found in each subject.

Figure 18 again shows the data for $AaDO_2$ versus PAO_2 as found in the Series One tests. A linear regression was performed on the hyperventilation and post-hyperventilation data separately thus approximately dividing the data into two ranges of PAO_2 above and below a PAO_2 of 95 mmHg.

Figure 18 also includes the results of the computer program for shunting values of 0, 2, and 5 percent of the total blood flow (the 0 percent shunt line being the horizontal axis for $AaDO_2$ equal to zero). The 2 percent shunt line presented an interesting fit to the data. It follows closely the two line fit to the data. For any given PAO_2 associated with an $AaDO_2$ from the data, the $AaDO_2$ predicted from the shunt line, the one line fit of Figure 12, and the two line fit of Figure 18 was found. This difference between the predicted and experimental values of $AaDO_2$ at a given PAO_2 represents the error between the data and the assumed fit. In considering the three different fits to the data, the average error of the data about the 2 percent shunt line was smaller than either the two line fit of

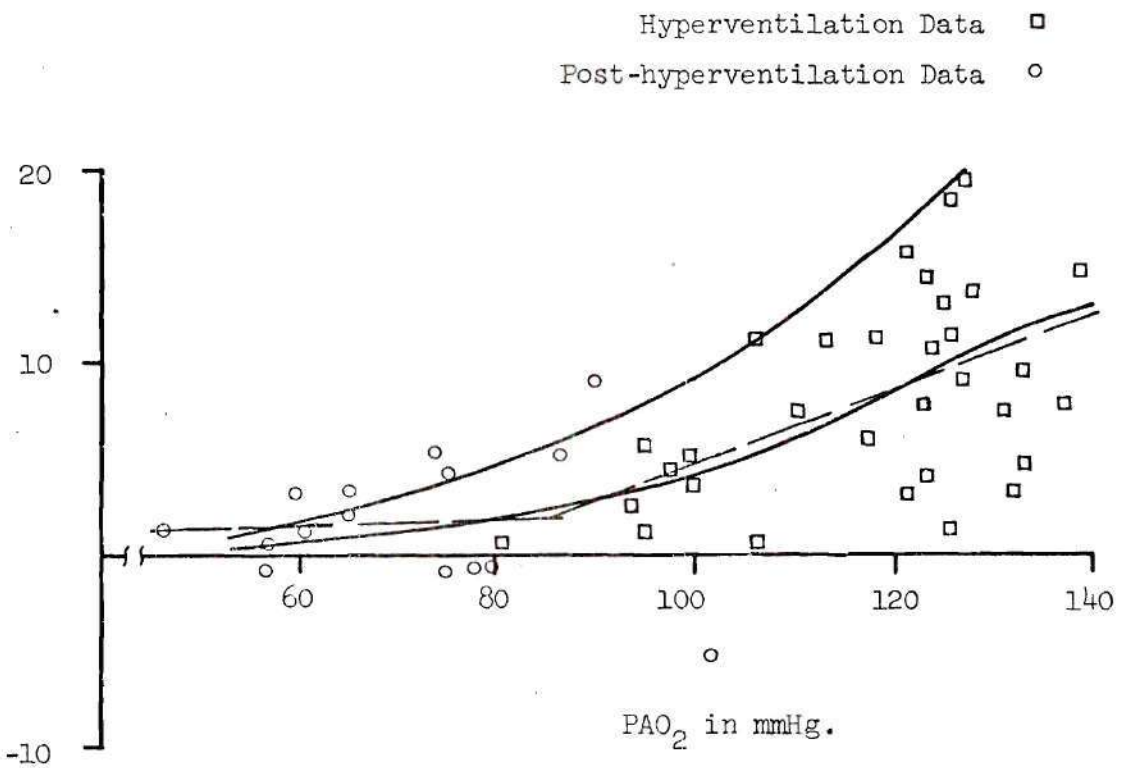

Figure 18. Effects of Shunting Displayed with Series One Data.

Figure 18 or the one line fit of Figure 12 (3.1 versus 3.3 and 3.4 mmHg average error respectively).

Figure 19 shows the results of four of the six subjects who had complete sets of data in the range of PAO_2 from 40 to 140 mmHg. Note that the data points for JKII and PR are scattered about the 4 percent shunt line and the data for FB and JE are scattered about the 1 percent shunt line. Figure 19 shows, then, the causes of some of the scatter shown in Figure 12. The cause of the scatter could be that each subject studied had different shunt sizes.

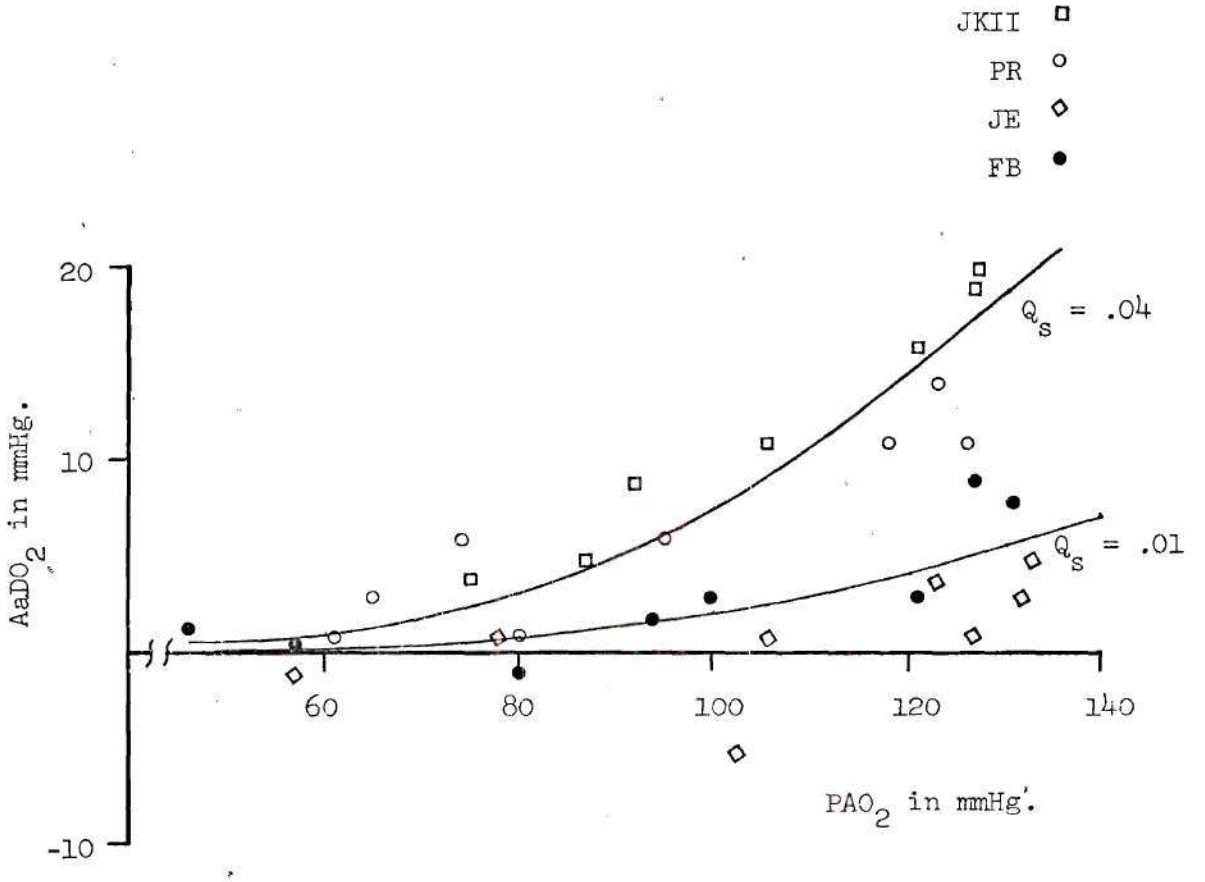

Figure 19. Effects of Shunting Displayed with Series One Data.

CHAPTER V

CONCLUSIONS

The purpose of the present study was to investigate the $AaDO_2$-$PACO_2$ and $AaDO_2$-PAO_2 relationships, and to determine if the $AaDO_2$ is controlled by the $PACO_2$. From the testing, the following conclusions were drawn:

1. With constant tidal volume, breathing rate, and PAO_2, the $PACO_2$ does not correlate well with the $AaDO_2$.

2. When the tidal volume, breathing rate, and PAO_2 are left free to vary, the $AaDO_2$ shows better correlation with the PAO_2 than with $PACO_2$.

3. The magnitude of the $AaDO_2$ at various levels of PAO_2 found in the present study can be explained by shunts ranging in size from 1 percent to 4 percent.

CHAPTER VI

RECOMMENDATIONS

The shape of the shunting curves in Figure 17 presents an interesting possibility. With increasing PAO_2, the $AaDO_2$ increases sharply to a plateau, then levels off. The magnitude of this $AaDO_2$ plateau depends on the magnitude of the shunt. This would yield the possibility of using the $AaDO_2$ to estimate the shunt size. In fact, as mentioned previously, at high FIO_2 the effects of time shunting and the shunt like characteristics of the $\dot{V}/\dot{Q}$ imbalance can be separated, and this value of $AaDO_2$ obtained can be attributed fully to true shunting. From this value of $AaDO_2$ and from a PvO_2 value, the entire curve due to true shunting can be reconstructed. Deviations from this curve shown by the subject at different levels of FIO_2 could then be attributed to $\dot{V}/\dot{Q}$ imbalance. This process would depend on the PvO_2 being constant over the range investigated. If there is a trend of increasing PvO_2 with increasing FIO_2 or PAO_2, the relationship noted could be incorporated into the program.

Lenfant (7) in his studies found that his subjects did indeed reach a $AaDO_2$ plateau, but at very high values of FIO_2 (near 100 percent oxygen), the $AaDO_2$ began dropping. Using the shunting model, the only possibility would seem to be a sharp increase in the PvO_2. If this sharp increase is not found, some factor other than true shunt must be sought to explain this sudden drop in $AaDO_2$ at high values of FIO_2.

The shunting model put forth is just one step in modeling the $AaDO_2$ in a human. For the purpose of this model, the contribution to the $AaDO_2$ from a $\dot{V}/\dot{Q}$ imbalance was neglected. The next step, would be the modeling and simulation of the $AaDO_2$ due to $\dot{V}/\dot{Q}$ imbalance and combining this model to that for shunting.

APPENDIX I

Referring to Figure 6 of the text, the problem of modeling becomes one of considering a front of Gas A moving down the tube with a different Gas B in front of it. Under the assumption of Hagan-Poiseuille flow, it is known that

$$u(r) = \frac{1}{4\mu} \frac{dP}{dl} (R^2 - r^2) \tag{1}$$

where μ is the viscosity and $u(r)$ is the velocity profile.

The maximum velocity (u_0) exists at the middle of the profile ($r = 0$), or

$$u_0 = \frac{1}{4\mu} \frac{dP}{dl} (R^2) \tag{2}$$

and the average velocity ($\bar{u}$) is

$$\bar{u} = \frac{R^2}{8\mu} \frac{dP}{dl} \tag{3}$$

The volumetric flow rate (Q) can be defined as

$$Q = \pi R^2 \bar{u} = \frac{\pi R^4}{8\mu} \frac{dP}{dl} \tag{4}$$

or integrating

$$Q = \frac{\pi R^4}{8\mu} \frac{(P_1 - P_2)}{L} \tag{5}$$

The mass flow rate, W, can be seen to be

$$W = \rho_{avg} Q = \frac{P_1 + P_2}{2R_c T} \frac{\pi R^4}{8\mu} \frac{(P_1 - P_2)}{L} \tag{6}$$

or

$$W = \frac{\pi}{16} \frac{R^4}{R_c T} \frac{(P_1^2 - P_2^2)}{L} \tag{7}$$

where R_c is the gas constant for that gas, T is the temperature, P_1 and P_2 are the upstream and downstream pressures respectively, and L is the length of the capillary.

Assuming the downstream pressure is zero, the mass flow rate at any point in the capillary can be written as

$$W = \frac{\pi R^4}{16\mu R_c T} \frac{P^2}{l} \tag{8}$$

where P is the pressure at that point and l is the distance from that point to the end of the tube.

Equation (8) can be rewritten as

$$W = \frac{kR^4 P^2}{\mu l} \tag{9}$$

by letting

$$k = \frac{\pi}{16\ R_c\ T}$$

Now rearranging equation (9) and differentiating

$$\frac{dP}{dl} = \sqrt{\frac{W\mu}{k}}\ \frac{1}{2\sqrt{l}\ R^2} \tag{10}$$

Returning to equation (2) and substituting for dP/dl, u_o can be rewritten as

$$u_o = \frac{1}{8}\sqrt{\frac{W}{k\mu}}\ \frac{1}{\sqrt{l}} \tag{11}$$

The time necessary to travel a distance dl at a velocity u_o can be written as

$$dT = \frac{dl}{u_o} \tag{12}$$

Substituting u_o from equation (11) and integrating, equation (12) can be rewritten as

$$TL = \frac{\frac{16}{3}\ L^{\frac{3}{2}}}{\sqrt{\frac{W}{k\mu}}} \tag{13}$$

where TL is defined as the lag time. This is the time for the gas to reach the downstream end of the capillary tube. The variables in equation (13) are the length and the mass flow rate (which is a function of radius).

Equation (13) represents the time required for the gas molecules at the center of the velocity profile to reach the sample chamber. The time for gas molecules on the other portions of the velocity profile to reach the sample chamber can be written as (assuming no mixing down the tube)

$$T(r) = \frac{R^2}{R^2 - r^2} TL$$

or

$$T(r) = \frac{TL}{1-\left(\frac{r}{R}\right)^2} \tag{14}$$

When 90 percent of the gas reaching the sample chamber is the new gas A,

$$\frac{\pi r^2}{\pi R^2} = .90$$

or

$$\frac{r^2}{R^2} = .90 \tag{15}$$

Substituting equation (15) into equation (14), the rise time (TR) can be seen to be

$$TR = 10\ TL \tag{16}$$

If mixing occurs down the tube, equation (16) is no longer valid as equation (14) is no longer valid.

Taylor, (26,27) has shown that the distance between the 10 percent plane and the 90 percent plane in the velocity profile can be approximated by

$$I_T = 3.62 k_D^{\frac{1}{2}}\ t^{\frac{1}{2}} \tag{17}$$

where t is the time from injection of the second gas and k_D is the dispersion coefficient given by

$$k_D = \frac{R^2 u^2}{48D} \tag{18}$$

where D is the diffusion coefficient between two gases given by (Reference 28)

$$D = \frac{.0069\ T^{\frac{3}{2}}}{P(V_A^{\frac{1}{3}} + V_B^{\frac{1}{3}})^2} \left(\frac{1}{M_A} + \frac{1}{M_B}\right)^{\frac{1}{2}} \tag{19}$$

where T is the temperature in degrees Randine, P is the total system pressure in atmospheres, V_A and V_B are the molecular volumes of the mixing gases, and M_A and M_B are the molecular weights of the gases.

Using equation (17) as an approximation to the distance between the 0 percent and 90 percent plane, the transition zone length at the downstream end can be written as

$$L_T = 3.62 k_D^{\frac{1}{2}} TL^{\frac{1}{2}} \tag{20}$$

If the time for the gas at a distance L_T to reach the sample chamber is now considered, the response time can now be written as

$$TR = \frac{\frac{16}{3} L_T^{\frac{3}{2}}}{\sqrt{\frac{W\mu}{k}}} \tag{21}$$

Referring back to equation (13), equation (21) can be expressed as

$$TR = T_L \left(\frac{L_T}{L}\right)^{\frac{3}{2}} \tag{22}$$

which gives as analytical expression for rise time.

APPENDIX II

Series One Test Results

	PAO_2* in mmHg	PaO_2* in mmHg	$PACO_2$* in mmHg	$AaDO_2$* in mmHg
JK I	97	92	38	5
	99	94	36	5
	113	102	29	11
	117	111	24	6
	125	112	19	13
JK II	106	95	34	11
	121	105	27	16
	126	107	22	19
	127	108	20	20
	87	82	26	5
	75	71	32	4
	92	82	33	9
FB	94	92	43	2
	100	96	40	3
	121	118	26	3
	127	118	19	9
	131	124	13	8
	46	44	32	2
	57	56	39	1
	80	81	40	-1
RV	95	94	39	1
	110	103	32	7
	124	113	25	11
	128	115	18	14
	139	124	11	15
JR	123	116	30	8
	133	123	21	9
	137	130	16	8
	75	76	24	-1
	60	57	27	3
	65	63	31	2

*All values were rounded. The resulting $AaDO_2$ values were determined before the PAO_2 and PaO_2 were rounded resulting in round off errors in the above numbers for $AaDO_2$.

	PAO_2 in mmHg	PaO_2 in mmHg	$PACO_2$ in mmHg	$AaDO_2$ in mmHg
PR	80	79	46	1
	95	90	43	6
	118	107	32	11
	123	109	22	14
	126	115	26	11
	65	62	35	3
	61	60	41	1
	74	69	42	6
JE	106	106	38	1
	123	119	23	4
	125	123	20	1
	132	129	17	3
	133	128	13	5
	102	107	24	-5
	78	77	28	1
	57	58	29	-1

Series Two Test Results

	PAO_2 in mmHg	PaO_2 in mmHg	$PACO_2$ in mmHg	$AaDO_2$ in mmHg
SK	130	119	19	11
	130	120	25	10
	130	121	28	10
	127	117	37	10
JK I	130	113	19	17
	129	111	24	18
	129	117	27	12
	131	111	35	20
JK II	131	113	17	18
	129	113	25	16
	128	112	33	16
	128	111	37	17
FB	135	131	13	5
	131	123	22	8
	131	124	26	7
	130	126	30	4
	130	126	34	4
RV	130	115	17	15
	131	113	22	18
	130	121	29	9
	129	117	35	12
	128	117	44	11
JR	136	126	17	11
	137	125	21	12
	133	125	26	8
	133	126	33	7
	132	126	40	6
PR	125	109	20	16
	124	114	25	11
	118	108	32	10
	120	113	38	7
	118	108	45	10
JE	132	125	18	7
	131	125	24	6
	129	122	40	7
	132	123	44	9

APPENDIX III

```
DAVIS-J-A*JAD.SH
     1                REAL INIT,LIM
     2                DIMENSION PO2(400),TPAO2(400),E(400),SF(3),
     3               1AADO2(100,3)
     4                READ(5,1)LIM,BF,PVO2,INIT
     5                N=1
     6          1     FORMAT()
     7                READ(5,1)(SF(L),L=1,3)
     8          2     I=1
     9                PO2(I)=INIT
    10         44     CO2=20.84*((1-EXP(-.04*PO2(I)))*(1-EXP(-.08*PO2(I))))
    11               1**1.1+.003026*PO2(I)
    12                CVO2=20.84*((1-EXP(-.04*PVC2))*(1-EXP(-.08*PVO2)))**1.1
    13               1+.003026*PVO2
    14                TO2=CO2*BF*(1-SF(N))+CVO2*BF*SF(N)
    15                TCO2=TO2/BF
    16                J=1
    17         99     TPAO2(J)=PO2(I)-J
    18                CAO2=20.84*((1-EXP(-.04*TPAO2(J)))*(1-EXP(1.08*TPAO2(J)
    19               1)))**1.1+.003026*TPAO2(J)
    20                E(J)=TCO2-CAO2
    21                IF(E(J).GT.0.)GO TO 66
    22                J=J+1
    23                GO TO 99
    24         66     IF(ABS(E(J)).GT.ABS(E(J-1)))GO TO 55
    25                AADO2(I,N)=PO2(I)-TPAO2(J)
    26                GO TO 77
    27         55     AADO2(I,N)=PO2(I)-TPAO2(J-1)
    28         77     I=I+1
    29                PO2(I)=PO2(I-1)+10.
    30                IF(PO2(I).LE.LIM)GO TO 44
    31                M=I-1
    32                N=N+1
    33                IF(N.LE.3)GO TO 2
    34                WRITE(6,22)
    35         22     FORMAT(5HOPAO2,5X,37HQS=FRACTION OF TOTAL CARDIAC
                         OUTPUT)
    36                WRITE(6,23)SF
    37         23     FORMAT(7X,3(3X,3HQS=,F3.2))
    38                WRITE(6,19)
    39         19     FORMAT(6X,3(4X,5HAADO2))
    40                DO 25 I=1,M
    41                WRITE(6,25)PO2(I),(AADO2(I,N),N=1,3)
    42         25     FORMAT(F6.1,1X,3(5X,F4.0)
    43                STOP
    44                END
END PRT≠
```

```
DXQT JAD.SH

DATA

PAO2        QS = FRACTION OF TOTAL CARDIAC OUTPUT
            QS = .02      QS = .03      QS = .05      QS = .10
            AADO2         AADO2         AADO2         AADO2
 80.0          2.            3.            4.            8.
 90.0          3.            4.            7.           12.
100.0          4.            6.            9.           16.
110.0          6.            9.           13.           22.
120.0          8.           12.           17.           28.
130.0         11.           15.           22.           35.
140.0         13.           19.           27.           42.
150.0         16.           23.           33.           50.
160.0         19.           27.           39.           57.
170.0         22.           31.           44.           65.
180.0         25.           35.           50.           73.
190.0         27.           39.           56.           81.
200.0         30.           42.           61.           89.
210.0         31.           45.           66.           97.
220.0         33.           47.           71.          104.
230.0         34.           49.           75.          112.
240.0         35.           51.           79.          119.
250.0         35.           52.           82.          127.
260.0         36.           53.           85.          134.
270.0         36.           54.           87.          141.
280.0         37.           55.           89.          147.
290.0         37.           55.           90.          153.
300.0         37.           56.           91.          159.
310.0         37.           56.           93.          165.
320.0         38.           56.           93.          170.
330.0         38.           57.           94.          174.
340.0         38.           57.           95.          179.
350.0         38.           57.           95.          182.
360.0         38.           58.           96.          185.
370.0         39.           58.           97.          188.
380.0         39.           58.           97.          191.
390.0         39.           59.           98.          193.
400.0         39.           59.           98.          194.
END     2862 MLSEC
```

LITERATURE CITED

1. Levine, G. et al. (1970) Gas Exchange Abnormalities in Mild Bronchitis and Asymptomatic Asthma. The New England Journal of Medicine. 282:1277-82.

2. Refsum, H. E. and Kim, B. M. (1967) The Alveolo-Arterial Oxygen Tension Difference at Varying Alveolar Ventilation in Patients with Pulmonary Disease Breathing Air. Clin. Sci. 33:569-76.

3. Riley, R. L. and Cournand, A. (1949) 'Ideal' Alveolar Air and the Analysis of Ventilation-Perfusion Relationships in the Lungs. J. Appl. Physiol. 1:825-47.

4. Bates, D. V., Macklem, P. T. and Christie, R. V. (1971) Respiratory Function in Disease. 60-75. Philadelphia: W. B. Saunders Company.

5. Riley, R. L. and Cournand, A. (1951) Analysis of Factors Affecting Partial Pressures of Oxygen and Carbon Dioxide in Gas and Blood of Lungs: Theory. J. Appl. Physiol. 4:77-101.

6. Ayres, S. M., Criscitiello, A. and Grabovsky, E. (1964) Components of Alveolar-Arterial O_2 Difference in Normal Man. J. Appl. Physiol., 19(1):43-47.

7. Lenfant, C. (1963) Measurement of Ventilation/Perfusion Distribution with Alveolar-Arterial Differences. J. Appl. Physiol. 18(6):1090-94.

8. Cole, R. B. and Bishop, J. M. (1967) Variation in Alveolar-Arterial O_2 Tension. J. Appl. Physiol. 22(4):685-93.

9. Cole, R. B. and Bishop, J. M. (1963) Effect of Varying Inspired O_2 on Alveolar-Arterial O_2 Tension Difference in Man. J. Appl. Physiol. 18:1043-48.

10. Farhi, L. E. and Rahn, H. (1955) A Theoretical Analysis of the Alveolar-Arterial O_2 to the Distribution Effect. J. Appl. Physiol. 7:699-703.

11. Rahn, H. and Farhi, L. E. (1964) Ventilation, Perfusion, and Gas Exchange - the V_A/Q Concept. Handbook of Physiology. 1(3):735-65.

12. Kim, B. M. and Refsum, H. E. (1968) Changes in Alveolar-Arterial Oxygen Tension Difference ($A\text{-}aDO_2$) During Variations in Alveolar Ventilation. Acta. Physiol. Scand. 73:36-41.

13. Pichotka, J. P. et al. (1971) Changes of the Alveolar-Arterial O_2 Pressure Difference. Pfluger's Archives. 327:53-67.

14. Fowler, K. T. (1969) The Respiratory Mass Spectrometer. Phys. Med. Biol. 14(2):185-99.

15. Lilly, J. C. (1950) Physical Methods of Respiratory Gas Analysis. Meth. in Med. Res. 2:131-37.

16. Siri, W. (1947) A Mass Spectroscope for Analysis in the Low Mass Range. The Review of Scientific Instruments. 18:540-45.

17. Hunter, J. A., Stacy, R. W. and Hitchcock, F. A. (1949) A Mass Spectrometer for Continuous Gas Analysis. The Review of Scientific Instruments. 20:333-36.

18. Nier, A. O. (1940) A Mass Spectrometer for Routine Isotope Abundance Measurements. Rev. Sci. Inst. 11:212-16.

19. Nier, A. O. (1947) A Mass Spectrometer for Isotope and Gas Analysis. Rev. Sci. Inst. 18:398-411.

20. Miller, F. A. et al. (1950) The Development of, and Certain Clinical Applications for, a Portable Mass Spectrometer. Vol. of Thoractic Surgery. 20:714-28.

21. Fowler, K. T. (1958) A Mass Spectrometer for the Rapid and Continuous Analysis of Gas Mixtures in Respiratory Research. (Ph.D. Thesis, University of London).

22. Muysers, K., Smidt, U. and Worth, G. (1967) Mass Spectrometry Applied to Lung Physiology, Bull. Physio. Path. Resp. 327-37.

23. Leeming, M. N. and Howland, W. S. (1959) Time Delay Technique in Respiratory Instrumentation. Respiration Physiology. 7:399-402.

24. Andersen, B. W. (1967) The Analysis and Design of Pneumatic Systems. 39-45. New York: John Wiley & Sons, Inc.

25. Collins, R. E. (1961) Flow of Fluids Through Porous Materials. New York: Reinhold Publishing Corp.

26. Taylor, G. (1953) Dispersion of Soluble Matter in Solvent Flowing Slowly Through a Tube. Proc. Roy. Soc. A219:186-203.

27. Taylor, G. (1954) Conditions Under Which Dispersion of a Solute in a Stream of Solvent Can Be Used to Measure Molecular Diffusion, Proc. Roy. Soc., A223:466.

28. Holman, J. P. (1968) Heat Transfer. 329. New York: McGraw-Hill Book Company.

29. Ganong, W. F. (1967) Review of Medical Physiology. 471. Los Altos: Lange Medical Publications.

30. Colquhoun, D. (1971) Lectures on Biostatistics. 214-278. London: Oxford University Press.

31. Murphy, T. W. (1966) A Two-Compartment Model of the Lung. Memorandum RM-4833-NIH, Jan. 1966. The Rand Corporation, 1700 Main Street, Santa Monica, Calif. 90406.

32. Slonim, N. B. and Chapin, J. L. (1964) Respiratory Physiology. 64-69. St. Louis: The C. V. Mosby Company.